

Rational Design, Synthesis, and Biological Evaluation of 7-azaindole Derivatives as Potent Focused Multi-Targeted Kinase Inhibitors

Bénédicte Daydé-Cazals, Bénédicte Fauvel, Mathilde Singer, Clémence Feneyrolles, Benoît Bestgen, Fanny Gassiot, Aurélia Spenlinhauer, Pierre Warnault, Nathalie Van Hijfte, Nozha Borjini, Gwénaél Chevé, and Aziz Yasri

J. Med. Chem., **Just Accepted Manuscript** • DOI: 10.1021/acs.jmedchem.6b00087 • Publication Date (Web): 24 Mar 2016

Downloaded from <http://pubs.acs.org> on March 26, 2016

Just Accepted

“Just Accepted” manuscripts have been peer-reviewed and accepted for publication. They are posted online prior to technical editing, formatting for publication and author proofing. The American Chemical Society provides “Just Accepted” as a free service to the research community to expedite the dissemination of scientific material as soon as possible after acceptance. “Just Accepted” manuscripts appear in full in PDF format accompanied by an HTML abstract. “Just Accepted” manuscripts have been fully peer reviewed, but should not be considered the official version of record. They are accessible to all readers and citable by the Digital Object Identifier (DOI®). “Just Accepted” is an optional service offered to authors. Therefore, the “Just Accepted” Web site may not include all articles that will be published in the journal. After a manuscript is technically edited and formatted, it will be removed from the “Just Accepted” Web site and published as an ASAP article. Note that technical editing may introduce minor changes to the manuscript text and/or graphics which could affect content, and all legal disclaimers and ethical guidelines that apply to the journal pertain. ACS cannot be held responsible for errors or consequences arising from the use of information contained in these “Just Accepted” manuscripts.

1
2
3
4
5
6
7 Rational Design, Synthesis, and Biological Evaluation of 7-azaindole
8
9
10 Derivatives as Potent Focused Multi-Targeted Kinase Inhibitors
11
12

13
14 *Bénédicte Daydé-Cazals, Bénédicte Fauvel, Mathilde Singer, Clémence Feneyrolles, Benoit*
15
16 *Bestgen, Fanny Gassiot, Aurélia Spenlinhauer, Pierre Warnault, Nathalie Van Hijfte, Nozha*
17
18 *Borjini, Gwénaél Chevé, Aziz Yasri**
19

20
21
22 OriBase Pharma, Cap Gamma, Parc Euromédecine, 1682 rue de la Valsière, CS 17383, 34189
23
24 Montpellier Cedex 4, France
25
26

27
28
29 **ABSTRACT**
30
31

32 Efforts were made to improve a series of potent dual ABL/SRC inhibitors based on a 7-azaindole
33
34 core with the aim of developing compounds that demonstrate a wider activity on selected
35
36 oncogenic kinases. Multi-Targeted Kinase Inhibitors (MTKIs) were then derived, focusing on
37
38 kinases involved in both angiogenesis and tumorigenesis processes. Anti-proliferative activity
39
40 studies using different cellular models led to the discovery of a lead candidate (**6z**) that combined
41
42 both anti-angiogenic and anti-tumoral effects. The activity of **6z** was assessed against a panel of
43
44 kinases and cell lines including solid cancers and leukemia cell models to explore its potential
45
46 therapeutic applications. With its potency and selectivity for oncogenic kinases, **6z** was revealed
47
48 to be a focused MTKI that should have a bright future in fighting a wide range of cancers.
49
50
51
52
53
54
55
56
57
58
59
60

INTRODUCTION

The modulation of kinase function is an important goal in drug discovery and, more particularly, in cancer-targeted therapies where an increased number of kinase inhibitors have entered the market in recent years.^{1,2} Two opposing concepts govern the design and development of new kinase inhibitors in oncology. While the first strategy proposes the design of selective molecules to increase efficacy and limit toxicity, the second strategy highlights benefits in developing Multi-Targeted Kinase Inhibitors (MTKIs). Although almost all major human cancers seem to harbor not a single but several concomitant dysregulations of kinase pathways, the latest approach offers the opportunity to catch tumor progression more effectively but also to avoid mechanisms of resistance commonly activated by the tumor to escape targeted therapies.^{3,4} Moreover, given that different types of tumors may originate from different cell types and are frequently driven by different combinations of genetic alterations, MTKIs will have the ability not only to be used in a wide range of cancers but will also prove to be as effective as combinatorial therapy without the disadvantages of using multiple selective agents together (drug-drug interactions, difficulty in obtaining sufficient potencies against the tumor cells, potentiation of adverse effects, etc.).⁵ Thus, kinase inhibitor development efforts in cancer therapy have shifted from the dogma of one molecule against one target for one disease to a more controlled multi-targeting with the aim of addressing the genetic diversity and multiple driving forces of disease.^{6,7} The three major groups of targets in the current kinase inhibitor drug discovery are receptor tyrosine kinases, kinases of the mitogen-activated protein kinase (MAPK) pathway and kinases of the phosphoinositide 3-kinase (PI3K) pathway. Because these three groups of targets are mechanistically linked, there is a compelling biological rationale for simultaneously targeting several members of each of these groups to create therapeutic benefits.

1
2
3 Using fragment-based drug design combined with medicinal chemistry approaches, we have
4 developed a new generation of type-II ATP-competitive MTKIs. The series was rationally
5 designed according to a structure-based drug design and kinase-focused approach to identify
6 single agents with an optimized multi-pharmacological inhibition profile. Recently, a series of
7 DFG-in inhibitors was first designed and evaluated against kinases of the ABL and SRC
8 families.^{8,9} Using these DFG-in inhibitors composed of a 7-azaindole core as the initial fragment,
9 followed by iterative structural and kinase activity improvements, we have identified new type-II
10 MTKIs that are highly potent against the ABL and SRC families but also on other oncogenic
11 kinase members of the receptor tyrosine kinase group and the MAPK pathway. Thus, the
12 compounds target multiple kinase pathways involved in tumor progression, angiogenesis,
13 immune system modulation and metastasis. This new series presents high anti-proliferative
14 activity, demonstrating the inhibition of the tumor cells, the angiogenesis process and more
15 broadly, an effect on the tumor microenvironment against a wide range of cancer types.
16 Moreover, with this multi-targeted profile, the compounds are expected not only to avoid
17 development of tumor resistance but also to be used as a therapeutic aid for patients developing
18 resistance while being treated with currently marketed kinase inhibitors.
19
20
21
22
23
24
25
26
27
28
29
30
31
32
33
34
35
36
37
38
39
40
41
42

43 **RESULTS AND DISCUSSION**

44 **Fragment-based drug design of 7-azaindole series**

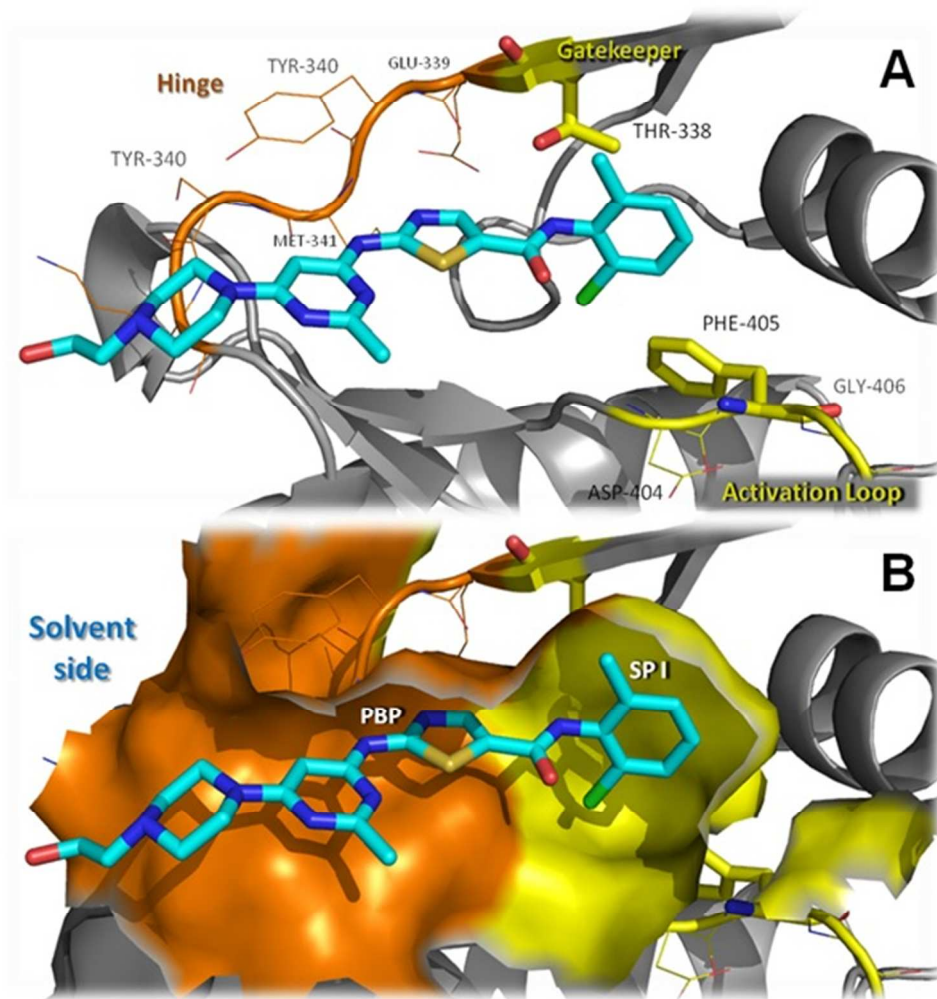
45
46 Two main strategies are used to design kinase inhibitors. The strategy adopted depends on the
47 targeted conformation of the kinase.
48
49
50

51 As depicted in Figure 1, the type-I inhibitors are designed to interact with the kinase in its
52 active or DFG-in conformation. In this strategy, a cyclic core (aromatic or not) is used to interact
53
54
55
56
57
58
59
60

1
2
3 with the segment linking the N-terminal to the C-terminal lobe of the kinase, therefore called the
4 hinge. A second fragment, usually an aromatic ring, is used to interact with a first specificity
5 pocket of the kinase that is separated from the hinge by a single amino acid called the
6 gatekeeper. As the gatekeeper presents an obstacle to the interaction with the specificity pocket
7 through steric hindrance, a linker is used between the aromatic ring and the cyclic ring system
8 interacting with the hinge to bypass this binding obstacle.
9
10
11
12
13
14
15
16

17
18 As depicted in Figure 2, the type-II inhibitors are designed to interact and block the kinase in
19 its inactive, or DFG-out, conformation. As in the DFG-in strategy, the interactions with the hinge
20 and the specificity pocket are found in type-II inhibitors. The difference lies in the exploration of
21 the rest of the kinase pocket. The aromatic fragment interacting with the first hydrophobic pocket
22 is extended *via* a linker (amide or urea) by another aromatic ring holding or not holding some
23 substituents. This last fragment is supposed to interact with a new hydrophobic pocket formed
24 after the structural rearrangement of the activation loop of the kinase. This second selective
25 pocket is the less conserved among the kinases and allows the establishment of more interactions
26 between the inhibitor and the active site and therefore increases the potency and the selectivity of
27 the inhibitor. The design of the type-II inhibitor strategy was then selected for the present work.
28
29 Our series of compounds is composed of a 7-azaindole core that is considered an adenine
30 mimetic heterocycle and is predicted to dock into the purine binding site by interacting with the
31 hinge. As shown in a previous study,⁸ the addition of a first aromatic ring (best with methyl-
32 substituted phenyl) to the 7-azaindole moiety with an aminomethyl linker allows interaction with
33 the first hydrophobic pocket juxtaposed to the gatekeeper existing both in the active or inactive
34 conformation. Accordingly, and to design selective type-II inhibitors, a second aromatic moiety
35 was added to the inhibitor structure to create new hydrophobic interactions with the second
36
37
38
39
40
41
42
43
44
45
46
47
48
49
50
51
52
53
54
55
56
57
58
59
60

1
2
3
4 specificity pocket. A docking study predicted that such compounds should adopt the classical
5
6 binding mode of type II-inhibitors such as Imatinib (Figure 2). An example of the superposition
7
8 of our compound **6x** docked to Imatinib co-crystallized ABL kinase is depicted in Figure 3 and
9
10 showed a similar type-II binding mode with at least 5 hydrogen bonds established within the
11
12 kinase active site.
13
14
15



50
51
52
53
54
55
56
57
58
59
60

Figure 1. Classical structural scheme of type-I kinase inhibitor docked into the DFG-in conformation. Example of Dasatinib co-crystallized within the SRC kinase (PDB: 3G5D¹⁰). A: Representation of the principal amino acids surrounding the ligand. B: View of the active site surface, PBP: Purine Binding Pocket, SP I: Selectivity Pocket I.

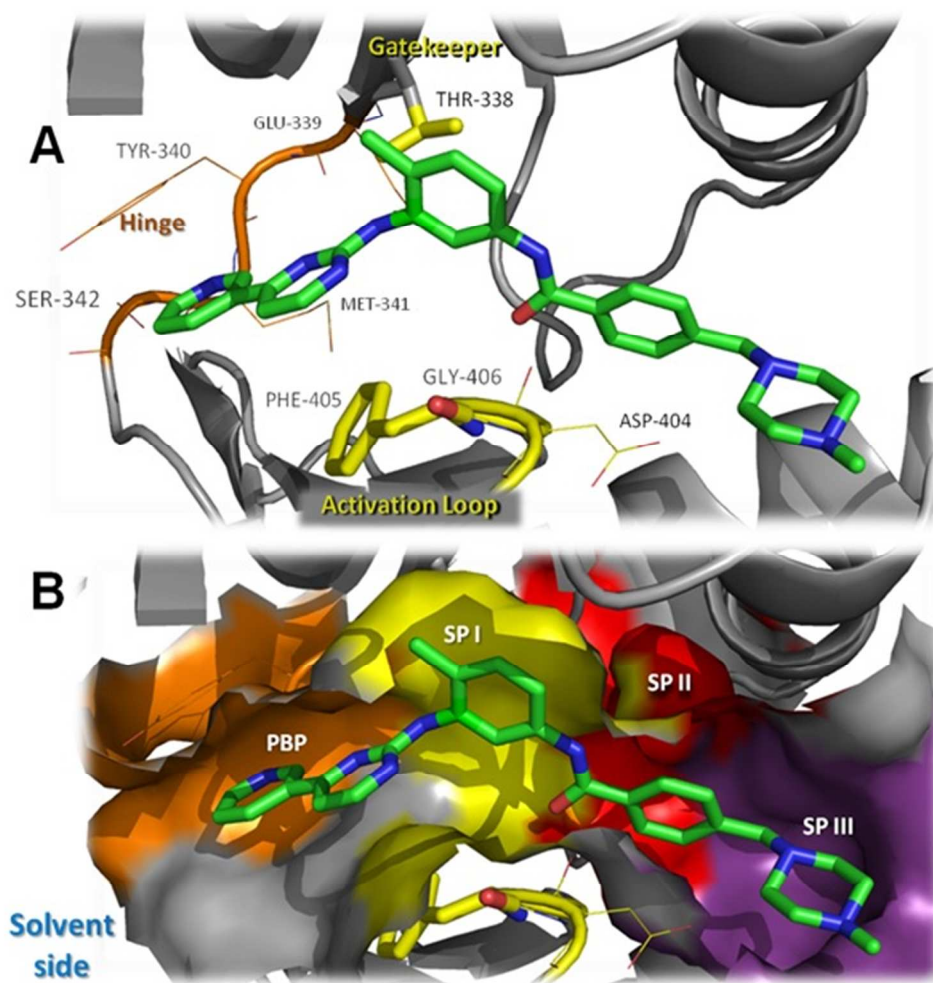


Figure 2. Classical structural scheme of a type-II kinase inhibitor docked into DFG-out conformation. Example of Imatinib co-crystallized within the SRC kinase (PDB: 2OIQ¹¹). A: Representation of the principal amino acids surrounding the ligand. B: View of the active site surface, PBP: Purine Binding Pocket, SP I: Selectivity Pocket I, SP II: Selectivity Pocket II, SP III: Selectivity Pocket III.

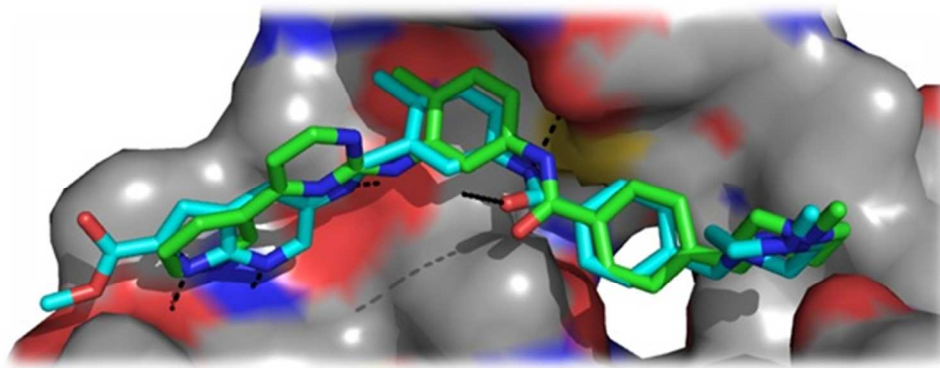


Figure 3. A. Superposition of the predicted binding mode of **6x** (in cyan) and Imatinib (in green) within the active site of ABL (in grey). Potential hydrogen bonds are depicted in black dashed lines. Docking studies were performed with ABL X-ray structure co-crystallized with Imatinib (PDB: 1IEP¹²).

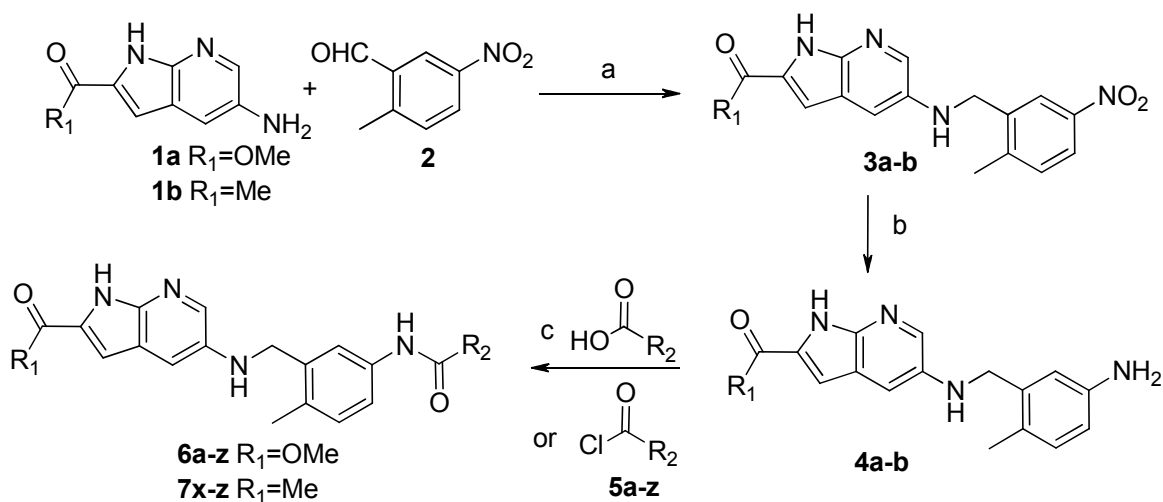
Medicinal Chemistry and Kinase Assays

Starting from the DFG-in series previously described,⁸ the aim was to design compounds able to inhibit kinases belonging to the receptor tyrosine kinase family, the SRC family and the MAPK pathway. We selected four representative kinases from the growth receptor tyrosine kinase family (EGFR, Epidermal Growth Factor Receptor; VEGFR2, Vascular Endothelial Growth Factor Receptor 2; FGFR2, Fibroblast Growth Factor Receptor 2; PDGFRA, Platelet-Derived Growth Factor Receptor Alpha), the SRC kinase as a member of the SRC family and the B-RAF kinase as one of the first kinases involved in the MAPK signaling pathway activation. Given the role of the specificity pocket in determining type-II inhibitor selectivity, chemical modulations were performed to explore different chemical fragments and their impact on the activity against the six targeted kinases.

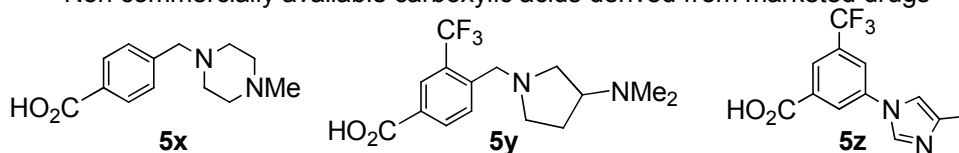
The general route of synthesis is described in Scheme 1. Compounds **6a-z** were obtained after a three-step synthesis from 5-amino-1*H*-pyrrolo[2,3-*b*]pyridine-2-carboxylic acid methyl ester

(**1a**), commercially available. After a reductive amination with 2-methyl-5-nitrobenzaldehyde (**2**) and sodium cyanoborohydride, the nitro-intermediate (**3a**) was reduced under hydrogen pressure and yielded the aniline intermediate (**4a**). To obtain the final compounds **6a-z**, the aniline (**4a**) was coupled with several carboxylic acids or acyl chlorides, commercially available **5a-w** or synthesized in house **5x-z** according to procedures described in the literature.^{13,14,15} Carboxylic acids and acyl chlorides **5a-w** are aromatic or heteroaromatic derivatives bearing hydrophobic or hydrophilic substituents in order to create potential interactions such as π -stacking or hydrogen bound with the second hydrophobic pocket of the kinase. The last carboxylic acids **5x-z** are fragments that were derived from marketed drugs (Imatinib, Bafetinib and Nilotinib, respectively) well known to interact with the specificity pocket of kinases such as ABL and/or SRC in its inactive conformation.

Scheme 1. Route of synthesis to explore the specificity pocket in the design of DFG-out type-II inhibitors^a



Non commercially available carboxylic acids derived from marketed drugs



^aReagents and conditions: (a) AcOH/MeOH (1/10), rt, 2 h, then NaBH₃CN, rt, 16 h-48 h, 82-86%; (b) H₂ (30 bars), Pd/C 10%, DMF or MeOH/HCl aq, rt, 16 h-48 h, 96-97%; (c) carboxylic acid, HATU, DIEA, rt, 12 h or acyl chloride, NEt₃, DMF, rt, 16 h, 4-55%.

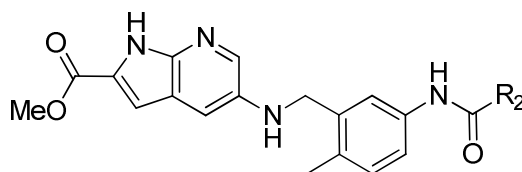
In this first series, a set of 26 compounds was synthesized and evaluated for their inhibition potency for targeted kinases at a concentration of 100 nM. As summarized in Table 1, this pharmacological assay resulted in a majority of compounds presenting at least 50% inhibition of SRC and PDGFRA kinase activities. These two kinases were slightly impacted by the nature of the substituent R₂. Inversely, with only two compounds (**6y** and **6z**) able to inhibit the FGFR2 kinase at more than 40% inhibition, this kinase likely adopts a more restrained type-II conformation. For the three other targets, B-RAF, EGFR and VEGFR2, no relevant correlation between the structure of the R₂ of the hydrophobic groups and the inhibition percentage of these kinases was observed.

Otherwise, when R₂ is a pyridine group, the nature and the position of the substituent as well as the position of the aromatic nitrogen atom with regard to the substitution (compounds **6m**, **6n**, **6o**, **6p**, **6q**) impact the inhibition profiles of the six kinases. Whatever the nature of the substituent (Me or CF₃), the 3-pyridine group allows an increase in the number of inhibited kinases by comparison with compounds bearing a phenyl group or a 4-pyridine group. For exemple, the nitrogen atom adjacent to the CF₃ group on the 4-pyridine ring leads to a less active compound (**6p**) whereas, with a 3-pyridine group, the compounds **6m** and **6o** inhibit five kinases. Globally, these results illustrated the difficulty of rationalizing the difference in the specificity profile observed among the 26 compounds on the targeted kinase panel. The 3-pyridine group would seem to be the best aromatic ring in R₂ position to have a MTKI profile and its combination with Imatinib and Bafetinib moiety would be interesting to test if the chemistry

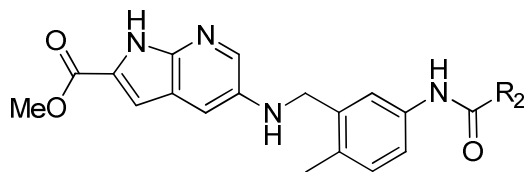
allows that. Based on these first findings, very interesting inhibition activities were observed for some of these compounds. Based on a value of 40% as an inhibition threshold, one compound (**6y**) showed a pan high inhibition of the six kinases, and one compound (**6z**) exhibited a moderate inhibition for the six kinases. Six compounds (**6m**, **6n**, **6o**, **6s**, **6u**, **6x**) inhibited five kinases except for FGFR2. Moreover, four compounds (**6a**, **6b**, **6j**, **6k**) inhibited four kinases and do not inhibit EGFR and FGFR2. The rest of the compounds inhibited 3 kinases or fewer and showed a heterogeneous inhibition profile.

These results allowed highlighting the MTKI potential of eight compounds (**6m**, **6n**, **6o**, **6s**, **6u**, **6x**, **6y**, **6z**), inhibiting at least five kinases of the selected primary kinase panel.

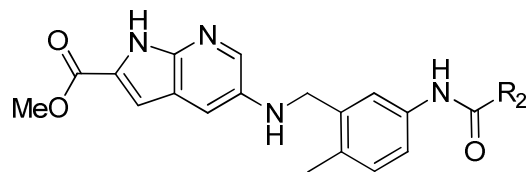
Table 1. Inhibition percentages at 100 nM for the first series of compounds



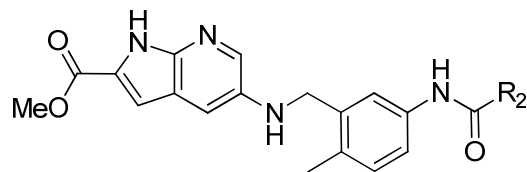
Compo und	R ²	Percent inhibition at 100 nM ^a					
		B-RAF	EGFR	FGFR2	PDGFRA	SRC	VEGFR2
6a		74%	32%	6%	87%	84%	72%
6b		63%	35%	1%	87%	85%	59%
6c		24%	52%	15%	61%	99%	32%



Compo und	R ²	Percent inhibition at 100 nM ^a					
		B-RAF	EGFR	FGFR2	PDGFRA	SRC	VEGFR2
6d		39%	63%	7%	68%	108%	38%
6e		29%	39%	8%	66%	105%	40%
6f		16%	64%	10%	47%	74%	19%
6g		11%	64%	5%	71%	86%	9%
6h		37%	53%	3%	74%	66%	36%
6i		14%	42%	5%	42%	108%	22%
6j		62%	16%	12%	93%	78%	42%



Compo und	R ²	Percent inhibition at 100 nM ^a					
		B-RAF	EGFR	FGFR2	PDGFRA	SRC	VEGFR2
6k		71%	-1%	8%	97%	65%	41%
6l		61%	2%	6%	87%	58%	29%
6m		95%	72%	19%	93%	89%	89%
6n		85%	49%	-6%	82%	51%	46%
6o		73%	78%	13%	93%	101%	73%
6p		-7%	32%	-2%	42%	42%	13%
6q		50%	81%	-7%	76%	39%	0%
6r		44%	2%	1%	85%	73%	33%



Compo und	R ²	Percent inhibition at 100 nM ^a					
		B-RAF	EGFR	FGFR2	PDGFRA	SRC	VEGFR2
6s		77%	40%	3%	91%	68%	58%
6t		69%	20%	4%	77%	34%	18%
6u		65%	45%	-4%	87%	59%	59%
6v		35%	66%	-1%	74%	72%	13%
6w		51%	15%	4%	71%	11%	37%
6x		60%	81%	21%	85%	93%	73%
6y		92%	80%	75%	90%	96%	96%
6z		54%	82%	52%	68%	49%	46%

1
2
3 ^a Mean of duplicate experiments. In the blue cells, the percent inhibition is superior to 40% at
4
5
6 100 nM.

7
8
9 In a set of pharmacomodulation experiments, the influence of the nature of the substituent on
10
11 the 7-azaindole core was investigated. The modifications focused on 1) replacing the methyl
12
13 ester group on position 2 of the 7-azaindole core by acetyl, *N*-methylester or carboxylic
14
15 functions or 2) changing the nature of the linker in position 5.

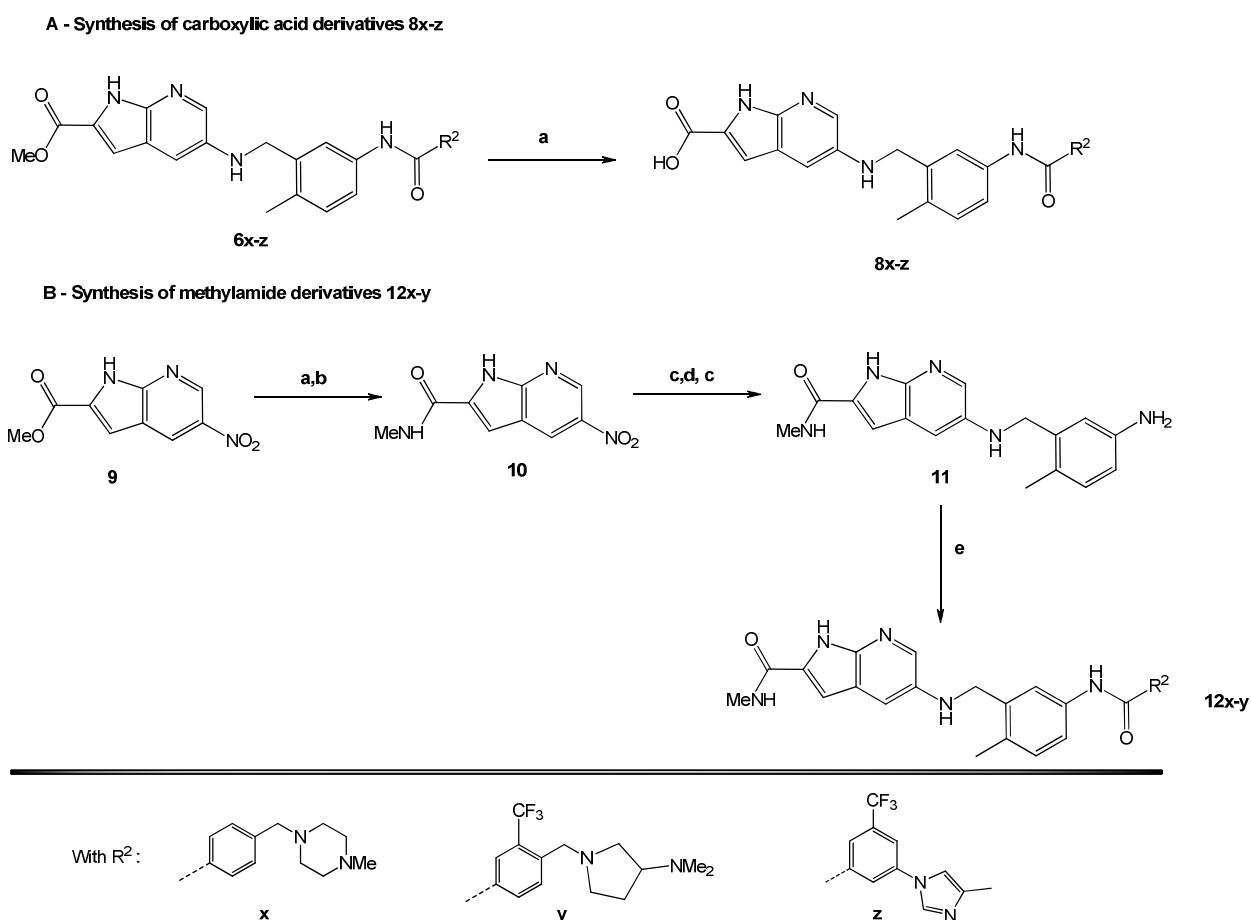
16
17
18 The first modifications in position 2 were introduced either by hydrolysis of the most active
19
20 compounds of the first series to afford the carboxylic derivatives **8x-z** (Scheme 2-A), or by using
21
22 the 1-(5-amino-1*H*-pyrrolo[2,3-*b*]pyridin-2-yl) ethanone (**1b**) bearing the acetyl group in position
23
24 2 to synthesize the acetyl derivatives **7x-z** according to the reaction pathway described in
25
26 Scheme 1 ($R_1 = \text{Me}$). Otherwise, the methyl ester function in position 2 of the 7-azaindole was
27
28 replaced by its corresponding *N*-methylester from 5-nitro-1*H*-pyrrolo[2,3-*b*]pyridine-2-
29
30 carboxylic acid methyl ester (**9**) in two steps to afford the new precursor **10**. This nitro
31
32 intermediate was reduced, and the corresponding aniline was used according to the same 3-step
33
34 synthesis strategy as for the first series (reductive amination, reduction by hydrogenation,
35
36 coupling reaction), as depicted in Scheme 2-B to prepare the methylester derivatives **12x-12y**.
37
38 This second series of compounds with modifications in position 2 of the 7-azaindole core was
39
40 screened on the six main targeted kinases for their inhibition potency at 100 nM concentration
41
42 and compared to their analogs in the methylester series (Table 2).

43
44
45 Some differences in the inhibition profile were observed regardless of the small variations
46
47 generated at position 2 of the 7-azaindole. Whatever the nature of the R_2 group, replacing the
48
49 methyl ester group by its corresponding carboxylic acid induces an important decrease of B-RAF
50
51 inhibition. Inversely, compounds with an acetyl substituent exhibit similar or better profiles than
52
53
54
55
56
57
58
59
60

the ester series. These results revealed the interest in working with the methyl ester and acetyl series in position 2 of the 7-azaindole core to optimize the series.

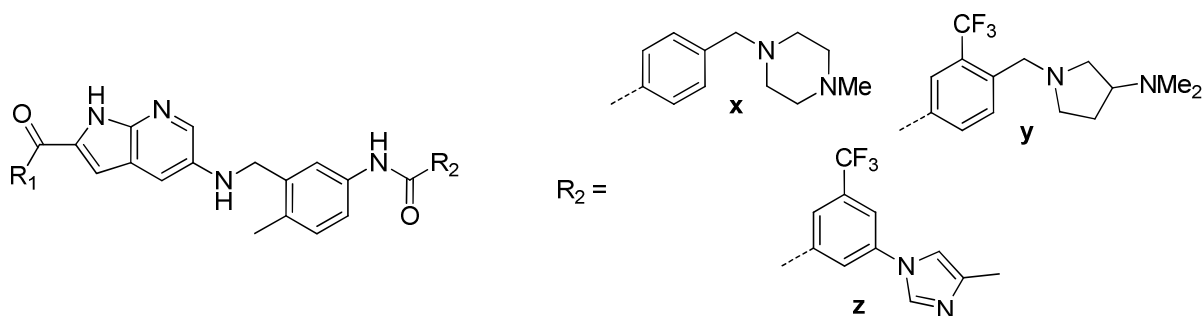
In parallel, several variations were performed in the position 5 of the 7-azaindole core to modify the linker bound to the central aromatic ring and to study the impact of five new linkers on the inhibition profile of the compounds. The chemistry investigated is depicted in Scheme 3.

Scheme 2. Synthesis pathway to modify the substituents on position 2 of the 7-azaindole core^a



^aReagents and conditions: (a) KOH or LiOH, MeOH/H₂O (1/1), reflux, 42-76%; (b) MeNH₂, HATU, DIEA, DMF, 59%; (c) H₂ (30 bars), Pd/C 10%, MeOH, overnight; (d) 2-methyl-5-nitrobenzaldehyde **2**, AcOH/MeOH (1/10), rt, 2 h then NaBH₃CN, rt, 16 h, overall yield for the three steps: 53%; (e) carboxylic acid, HATU, DIEA, DMF, rt, 16 h, 3-7%.

Table 2. Percent inhibition at 100 nM for compounds with modifications in position 2 of the 7-azaindole core.



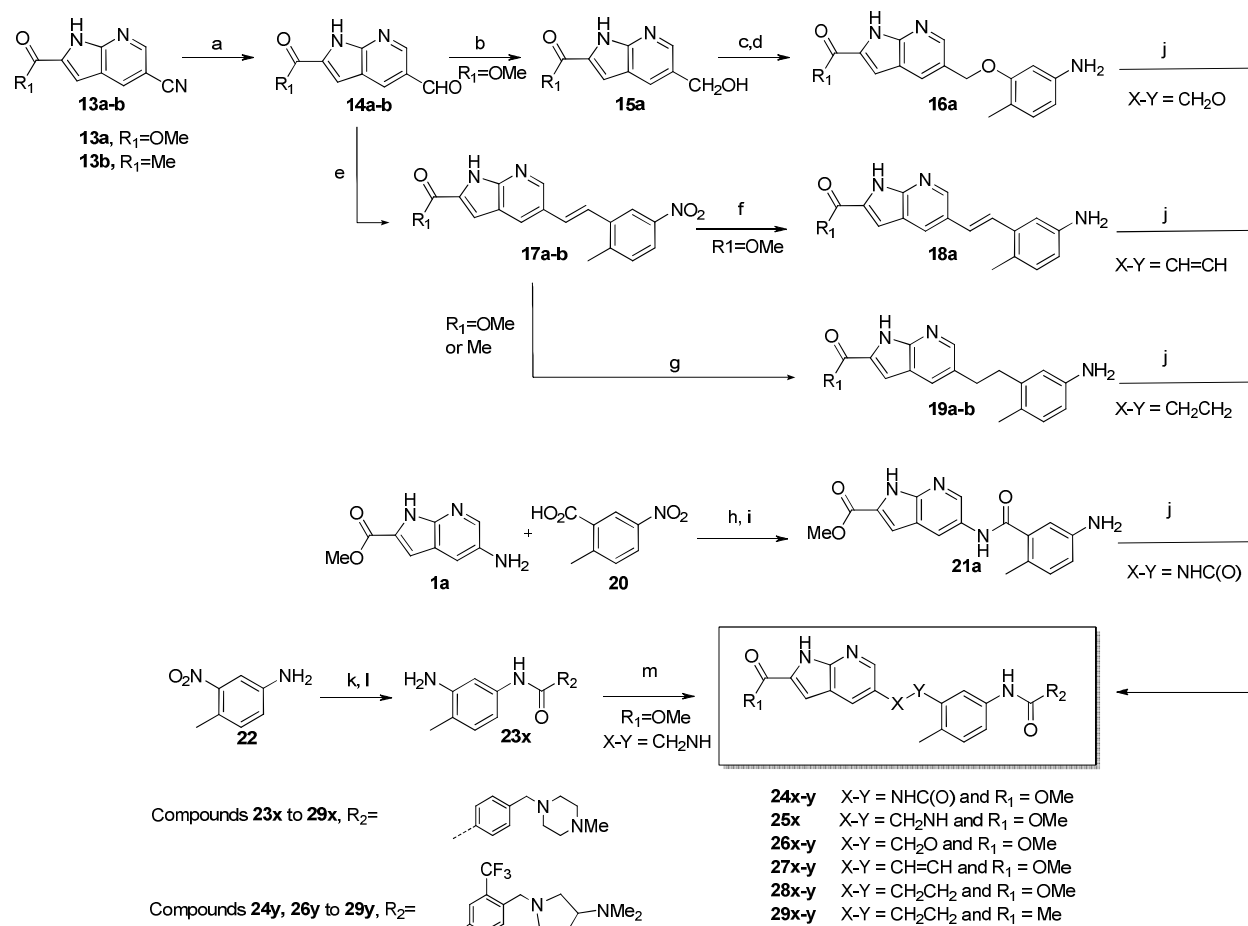
Compo und	Percent inhibition at 100 nM ^a							
	R ₁	R ₂	B-RAF	EGFR	FGFR2	PDGFRA	SRC	VEGFR2
6x	MeO	x	60%	81%	21%	85%	93%	73%
6y	MeO	y	92%	80%	75%	90%	96%	96%
6z	MeO	z	54%	82%	52%	68%	49%	46%
7x	Me	x	35%	99%	5%	96%	87%	88%
7y	Me	y	56%	94%	58%	73%	91%	71%
7z	Me	z	55%	43%	13%	24%	59%	24%
8x	HO	x	12%	96%	14%	79%	75%	72%
8y	HO	y	33%	98%	71%	66%	86%	80%
8z	HO	z	18%	91%	49%	63%	69%	58%
12x	MeHN	x	86%	99%	23%	95%	98%	93%
12y	MeHN	y	93%	101%	98%	94%	99%	87%

^a Mean of duplicate experiments. In the blue cells, the percent inhibition is superior to 40% at 100 nM.

1
2
3 The key intermediates used to introduce different linkers were the 5-formyl-1*H*-pyrrolo[2,3-
4 *b*]pyridine-2-carboxylic acid methyl ester (**14a**) and the 2-acetyl-1*H*-pyrrolo[2,3-*b*]pyridine-5-
5 carbaldehyde (**14b**) obtained, respectively from the 5-cyano-1*H*-pyrrolo[2,3-*b*]pyridine-2-
6 carboxylic acid methyl ester (**13a**) and the 2-acetyl-1*H*-pyrrolo[2,3-*b*]pyridine-5-carbonitrile
7 (**13b**). Whereas one reduction step with Raney nickel catalyst and hydrogen pressure was
8 sufficient in the ester series to obtain the aldehyde derivative **14a**, a supplementary step of
9 oxidation with manganese oxide was necessary in the acetyl series to obtain **14b** due to the
10 reduction of the acetyl group that occurred during the first reduction step. These two aldehyde
11 derivatives (**14a** and **14b**) allowed access to the final compounds **25d-k** with 3 different linkers
12 X-Y, either CH₂O, CH=CH or CH₂CH₂. To access compounds with the first cited ether linker
13 CH₂O, the aldehyde derivative **14a** was reduced with DIBAL-H reagent to its corresponding
14 alcohol (**15a**). This intermediate was used in a Mitsunobu reaction with 2-methyl-5-nitrophenol.
15 Then, a reduction of the nitro group followed by a peptide coupling reaction with the two
16 carboxylic acids **5x** and **5y** led to the final compounds **26x** and **26y**. A Wittig reaction was
17 performed using the aldehydes **14a** and **14b** with 2-methyl-5-nitrobenzyltriphenylphosphonium
18 to generate the intermediates **17a-b** with the alkene linker. These derivatives were partially or
19 completely reduced (step f or g, respectively) to derivatives **18a** or **19a-b** that were finally
20 coupled with the two carboxylic acids **5x** and **5y** to obtain the final compounds with an alkene
21 CH=CH (**27x-y**) or an alkyl linker CH₂CH₂ (**28x-y** and **29x-y**). Compounds **24x-y** with the
22 amide linker NHC(O) were obtained from 5-amino-1*H*-pyrrolo[2,3-*b*]pyridine-2- carboxylic acid
23 methyl ester **1a** and 5-amino-2-methyl-benzoic acid methyl ester **20** in three steps (coupling
24 reaction followed by nitro-reduction, then final coupling reaction). Finally, from 4-methyl-3-
25 nitroaniline **22**, a peptide coupling reaction followed by a reduction of the nitro group and a
26
27
28
29
30
31
32
33
34
35
36
37
38
39
40
41
42
43
44
45
46
47
48
49
50
51
52
53
54
55
56
57
58
59
60

reductive amination with **14a** led to the final derivative **25x** with the reverse amine linker CH_2NH .

Scheme 3. Synthesis pathway to modify the linker in position 5 of the 7-azaindole core^a

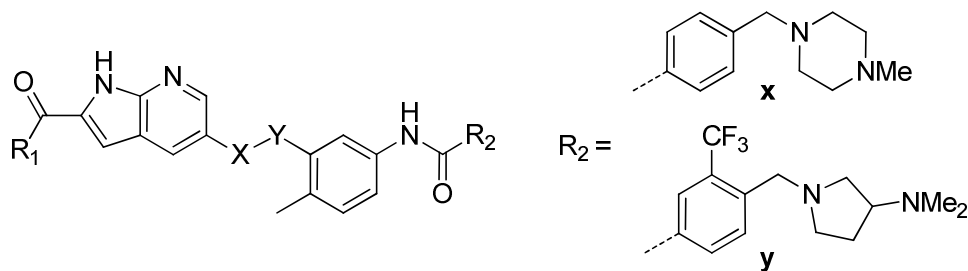


^aReagents and conditions: (a) **14a**: H₂ (10 bars), Raney Ni, Pyridine/H₂O/AcOH (2/1/1), overnight; 67%; **14b**: 1) DIBAL-H, toluene, 0°C, 1.5 h, 31%, 2) MnO₂, THF, rt, overnight, 65%; (b) DIBAL-H, THF, 0°C, 3 h, 45%; (c) 2-methyl-5-nitrophenol, PPh₃, DEAD, CH₂Cl₂, rt, overnight, 40%; (d) Zn, AcOEt/AcOH (2/1), 50°C, rt, 1 h 30; (e) 2-methyl-5-nitrobenzyl-triphenylphosphonium, LiOH, MeOH, rt or reflux, overnight, 69-71% **17b**; (f) Zn, AcOH/AcOEt (1/2), sonic bath, rt, 30 min, 56%; (g) H₂ (10 bars), Pd/C 10%, DMF, rt, 24 h, 26%-38%; (h)

HATU, DIEA, DMF, rt, w-end, 93%; (i) H₂ (35 bars), Pd/C 10%, MeOH, rt, overnight, 81%; (j) **5x** or **5y**, DIEA, HATU, DMF, rt, overnight, 5-55%; (k) **5x**, DIEA, EDCI, rt, overnight, 45%; (l) Zn, AcOEt/AcOH (2/1), rt, 1 h 20, quant. yield; (m) 1) **14a**, AcOH/MeOH (10/1), rt, 2 h, 2) NaBH₃CN, rt, overnight, 17%.

A total of eleven new compounds (**24** to **29**) were synthesized bearing 5 new linkers, and their inhibition profile was evaluated on the six targeted kinases and compared to their analogs with the initial linker NHCH₂.

Table 3. Inhibition percentages at 100 nM for compounds with modifications on position 5 of the 7-azaindole core.



Percent inhibition at 100 nM^a

Compound	R ₁	X-Y	R ₂	B-RAF	EGFR	FGFR2	PDGFRA	SRC	VEGFR2
6x	MeO	NHCH ₂	x	60%	81%	21%	85%	93%	73%
6y	MeO	NHCH ₂	y	92%	80%	75%	90%	96%	96%
24x	MeO	NHC(O)	x	71%	65%	8%	41%	94%	97%
24y	MeO	NHC(O)	y	46%	76%	94%	94%	100%	93%
25x	MeO	CH ₂ NH	x	17%	63%	8%	88%	47%	46%
26x	MeO	CH ₂ O	x	7%	81%	14%	98%	58%	67%

26y	MeO	CH ₂ O	y	15%	93%	69%	96%	87%	86%
27x	MeO	CH=CH	x	24%	38%	2%	88%	40%	51%
27y	MeO	CH=CH	y	33%	59%	38%	68%	55%	61%
28x	MeO	CH ₂ CH ₂	x	-19%	98%	35%	99%	91%	98%
28y	MeO	CH ₂ CH ₂	y	64%	97%	101%	105%	101%	102%
7x	Me	NHCH ₂	x	35%	99%	5%	96%	87%	88%
7y	Me	NHCH ₂	y	56%	94%	58%	73%	91%	71%
29x	Me	CH ₂ CH ₂	x	67%	86%	18%	86%	77%	92%
29y	Me	CH ₂ CH ₂	y	60%	83%	81%	89%	97%	99%

^a Mean of duplicate experiments. In the blue cells, the percent inhibition is superior to 40% at 100 nM.

The pharmacomodulations with the reverse amine linker (CH₂NH) or the alkene (CH=CH) linker induce an important decrease of the activity on the targeted kinases, excluding PDGFRA for which the modifications that were used slightly affect the inhibition of this kinase. For the other new tested linkers (NHC(O), CH₂O or CH₂CH₂), similar MTKI profiles were obtained on the targeted kinases when compared with compounds bearing the initial linker NHCH₂ except for B-RAF. Indeed, B-RAF kinase inhibition was the most negatively affected by the nature of the linker (decrease of the activity for 8 compounds over the 11 new ones). The best inhibition profiles were obtained for compounds bearing linkers NHCH₂ and CH₂CH₂. This new series of variations on position 5 of the 7-azaindole allowed highlighting the MTKI potency of six new compounds: **24x**, **24y**, **26y**, **28y**, **29x**, **29y**. These derivatives inhibited at least 5 of 6 targeted kinases with at least a 40% inhibition at 100 nM as the compounds **6x**, **6y**, **7y**.

Cellular Anti-Proliferative Effects of Compounds

The six targeted kinases are members of different signaling pathways involved in tumor growth and progression, including angiogenesis and metastasis processes. To validate the dual mechanism of action of the nineteen best compounds inhibiting at least 5 of 6 targeted kinases developed to date, their anti-proliferative potency was evaluated in a first screening experiment on human primary endothelial cells (HUVEC; Human Umbilical Vein Endothelial Cells) to prove the antiangiogenic effect and on a hepatocellular carcinoma cell line (HepG2) for the anti-tumoral activity of the compounds. In parallel, Sorafenib, a marketed MTKI approved by the FDA in the treatment of liver cancer, was incubated with cells and used as a reference compound. While presenting a good profile of kinase inhibition, **8y** and **8z** were not evaluated in cellular assays. We previously observed a lack of anti-proliferative activity for other DFG-out inhibitors bearing, as compounds **8y** and **8z**, a carboxylic acid in position 2 of the 7-azaindole. The EC50 on cells for different carboxylic compounds of this series could not have been calculated because no inhibition of proliferation was observed even at the highest evaluated concentrations of 3 μ M, indicating an EC50 at least 10-fold the EC50 of corresponding methylester compounds. Consequently, for this series, the presence of the carboxylic acid would avoid cell membrane penetration and thus would not allow such compounds to demonstrate anti-proliferative activity.

Table 4. Anti-proliferative effects of compounds represented by their EC₅₀ values on the HUVEC primary cells and the HepG2 cancer cell line.

		EC ₅₀ (nM)																
	Ref ^a	6m	6n	6o	6s	6u	6x	6y	6z	7y	12x	12y	24x	24y	26y	28y	29x	29y
HUVEC	718	>1000	986	390	298	199	>1000	689	34	97	>1000	83	>1000	631	426	171	118	163
HepG2	302	510	>1000	963	>1000	>1000	>1000	673	38	275	>1000	179	>1000	977	>1000	>1000	>1000	248

^aReference: Sorafenib.

While three compounds (**6x**, **12x** and **24x**) have failed to demonstrate any activity on HUVEC and HepG2 (concentration of compound superior to 1 μ M is needed to obtain a 50% inhibition of the cell proliferation), the other compounds exhibit good to excellent activity on at least one cell type as described in Table 4. With seven compounds showing both anti-proliferative and anti-angiogenic activities, four of the compounds out-performed Sorafenib (**6z**, **7y**, **12y**, **29y**). These four new leads were subjected to a second cellular screening approach aiming to confirm and compare them in terms of anti-proliferative activities on another type of endothelial cells (HRMEC; Human Retinal Microvascular Endothelial Cells) and two other human cancer cell lines (A549, a non-small cell lung cancer cell line and HT29, a colorectal cancer cell line). Erlotinib and Regorafenib were selected as reference compounds for lung and colorectal cancer cell lines, respectively, and demonstrated weak anti-proliferative activities. These new assays confirmed previous findings revealing new anti-proliferative effects on lung and colorectal cell lines. The compound **6z** showed the best anti-proliferative and anti-angiogenic effects with EC₅₀ lower than 70 nM on each cell type (Table 4 and 5). Demonstrating high *in cellulo* anti-angiogenic and anti-tumoral potency, **6z** was thus selected as our most promising lead compound for further *in vitro* development.

Table 5. Anti-proliferative effects of compounds represented by their EC₅₀ values on the HRMEC primary cells and the A549 and HT29 cancer cell lines.

	EC ₅₀ (nM)						
	6z	7y	12y	29y	Sorafenib	Erlotinib	Regorafenib
A549	64	204	495	293	>1000	>1000	>1000
HT29	37	150	227	303	>1000	>1000	>1000
HRMEC	62	179	81	304	>1000	>1000	nd ^a

^a nd: not determined.

Selectivity profile of **6z**

To assess the kinase selectivity profile of **6z**, a broad panel kinase screening was conducted using a biochemical enzymatic assay by evaluating the ability of the compound to inhibit kinases at a 100 nM concentration (Table 6). In these studies, **6z** was found to be a multi-targeted inhibitor with inhibition superior to 40% against 34 kinases of 104 kinases tested. The main kinases targeted by **6z** are important clinical targets in a variety of malignancies and support the therapeutic potential of **6z** as a broad anti-tumor agent. Kinases such as the Aurora kinase family or the Polo-like kinase 1 (PLK1) whose inhibition may have negative and particularly adverse effects (i.e., bone marrow suppression and neutropenia) were not inhibited by the compound. Moreover, **6z** is active on mutated kinases such as different ABL mutants involved in leukemia resistance, the well-known B-RAF mutant involved in melanoma and the mutation T790M of EGFR that is involved in the resistance of cells to anti-EGFR therapies in lung cancer. An IC₅₀ inferior or close to 50 nM was observed on ABL WT, ABL^{G250E}, ABL^{Y253F}, ABL^{E255K} and SRC, historically the first kinases targeted by this compound. As an MTKI, **6z** presents IC₅₀ values less than 50 nM against at least EGFR WT, LYN A, HCK, PDGFRA, YES, and B-RAF^{V600E}

(Table 7). These results confirm that our approach allows the selective design of MTKI compounds targeting only oncogenic kinases.

Table 6. Kinase inhibition profile of **6z** for a broad panel of kinases

Percent inhibition values of the kinase activity at 100 nM

% < 40			40 ≤ % < 80	% ≥ 80
ABL ^{T315I}	FGFR1	PI3K α	c-SRC	ABL WT
AKT2	GSK3b	PIM1	ARG	ABL ^{E255K}
AMPK	IGF-1R	PKA	B-RAF	ABL ^{G250E}
Aurora A	IKK beta	PKCa	BTK	ABL ^{Y253F}
Aurora B	IKK alpha	PKCd	CSK	BLK
Aurora C	INSRR	PKCe	EGFR ^{T790M}	BMX
AXL	ITK	PKCg	EPHA1	EGFR WT
CaMKII d	JAK2	PKC θ	EPHA2	EPHB2
CDK1/Cyclin B	JAK3	PKD2	EPHA4	FGR
CDK2/Cyclin A	MEK1	PLK1	EPHB4	HCK
CDK5/p25	ERK2	ROCKII	ERBB4	LCK
CDK7/CyclinH/MNAT1	MAPKAPK2	ROS1	FGFR2	LYN A
Cdk9/cyclin T1	MAPKAPK5	SYK	FLT3	YES
CHK2	MATK	TEC	CSF1R	B-RAF ^{V600E}
CK1	MST1R	TIE2	FRK	
c-KIT	mTOR	TRKA	FYN	
c-MER	MLCK	TSSK2	p38 alpha	
c-MET	NEK2	TYK1	PDGFRA	

DMPK	NUAK1	TYK2	RET
ERBB2	p70S6K	TYRO3	VEGFR2
FAK	PAK2	VEGFR1	
FER	PDGFRb	VEGFR3	
FES	PDK1	ZAP70	
	PHKG2		

Table 7: IC₅₀ value of **6z** on selected kinases inhibited with percent inhibition superior to 40% at 100 nM

Kinases	IC ₅₀ (nM)	Kinases	IC ₅₀ (nM)
ABL WT	6	PDGFRA	50
B-RAF ^{V600E}	10	ABL ^{Y253F}	51
EGFR WT	15	FRK	62
HCK	22	LCK	69
LYN A	37	ABL ^{E255K}	73
c-SRC	40	EGFR ^{T790M}	112
YES	44	FYN	131
ABL ^{G250E}	46		

Broad anti-proliferative effects of **6z**

Finally, we evaluated the therapeutic potential of **6z** against different types of cancers. The anti-proliferative effect of **6z** was compared to different reference compounds that are currently approved agents in the indication of interest or under evaluation in clinical trial phases. With the

MTKI profile of **6z** and its ability to inhibit clinically validated oncogenic kinases in almost all if not all types of cancer, we used either sensitive cancer cell lines or resistant/aggressive cells. The cells that were considered as sensitive are the BxPC-3 and Caki-2 cell lines which, respectively, represent human pancreatic and kidney cancer and the murine BaF3 WT leukemia-derived cell line expressing the human BCR-ABL wild-type fusion protein that is used as a model for the Philadelphia chromosome (Ph)-positive leukemias. PC-3 (human non-hormone-dependent prostate cancer cell line), MDA-MB-231 (triple-negative breast cancer cell lines), NCI-H1975 (non-small cell lung cancer cell line harboring the genetic modification of EGFR leading to the expression of a protein with L858R and T790M double mutations) and BaF3 T315I (the murine leukemia-derived cell line expressing the well-known mutated form of BCR-Abl fusion protein) were selected as representative of resistant and/or aggressive cancer cells.

Table 8: Anti-proliferative effects of **6z** in comparison with reference compounds represented by their EC₅₀ values on different cancer cell lines.

	EC ₅₀ (nM) ^a						
	PC-3	Caki-2	MDA-MB-231	BxPC-3	NCI-H1975	BaF3 WT	BaF3 T315I
6z	152	22	158	35	104	0.04	1.8
Dasatinib	232	55	44	33	173	0.04	>1000
Erlotinib	>1000	>1000	>1000	>1000	>1000	nd ^a	nd
Sunitinib	>1000	>1000	>1000	>1000	>1000	nd	>1000
Ponatinib	>1000	653	483	544	>1000	0.05	0.3
Imatinib	nd	nd	nd	nd	nd	34	>1000
Sorafenib	nd	>1000	>1000	>1000	>1000	nd	nd

1
2
3 **Afatinib** nd nd >1000 >1000 116 nd nd
4
5

6 ^a nd: not determined. In the grey cells, marketed references currently approved in the
7
8 indication.

9
10
11 EC50 values presented in Table 8 demonstrate that **6z** is highly cytotoxic with similar or even
12
13 better potency than reference compounds against a large panel of cancer cell types even if
14
15 aggressive or resistant.
16
17

18 19 20 21 **Pharmacokinetic profile of 6z in mice**

22
23 The pharmacokinetic (PK) parameters of **6z** were assessed in mice following intravenous (IV)
24
25 and oral (PO) administrations as described in Table 9. After IV administration at a dose of 2
26
27 mg/kg, the maximum concentration (C_{\max}) reached 853 ng/mL and the area under the curve
28
29 ($AUC_{0-\infty}$) was 558 ng/mL*h. After oral administration at 20 mg/kg, the C_{\max} reached 610 ng/mL
30
31 (1.1 μ M) at 0.5 h post-dosing and the $AUC_{0-\infty}$ was 3029 ng/mL*h (5.4 μ M*h).
32
33

34
35 These results demonstrate good PK properties of **6z** in mice with high oral bioavailability (close
36
37 to 47%) and a sustained plasma concentration exceeding *in vitro* EC_{50} during at least 8 hours
38
39 after oral dosing. These data indicate a favorable pharmacokinetic profile of **6z** in preparation for
40
41 efficacy studies in mice.
42
43

44
45 **Table 9:** Pharmacokinetic profile of **6z** in mice after IV and PO dosing

46
47

	Administration	Dose	C_{\max}	T_{\max}	$AUC_{0-\infty}$	F
	route	(mg/kg)	(ng/mL)	(h)	(ng/mL*h)	(%)
6z	IV	2	853	0.167	558	N/A ^a
	PO	20	610	0.500	3029	47

48
49
50
51
52
53
54
55
56
57 ^a N/A: not applicable
58
59
60

***in vitro* hERG patch clamp assay**

Blockade of the cardiac ion channel coded by human ether-à-gogo-related gene (hERG) can lead to cardiac arrhythmia, which has become a major concern in drug discovery and development, and mainly in the field of kinase inhibitors. The inhibitory effect of **6z** on the hERG channel was assessed using conventional patch clamp experiments. With very modest inhibition of hERG channel (26% inhibition at a 30 μ M concentration), the compound **6z** bears a minor risk of potentially problematic cardiac side-effects.

***in vitro* cytotoxicity effect of 6z on human activated and resting PBMC**

Several *in vitro* methods have been suggested to predict drug-induced haematotoxicity.^{16,17} We used primary cells (PBMC) isolated from peripheral blood from two healthy donors to assess and detect drug sensitivity in a short-term assay. Cells were exposed to increasing concentrations of **6z** or Dasatinib. Dasatinib was used as reference because it is the most similar compound to **6z** in term of anti-proliferative activity as observed on cancer cell lines (Table 8) and its immunosuppressive activity was demonstrated in patients.¹⁸ When PBMC were stimulated with phytohemagglutinin (PHA) supplemented with IL-2 (PHA/IL-2), mitogen/cytokine combination used widely to induce cell division, the EC₅₀ of **6z** and Dasatinib were close to 4.8 μ M and 2.4 μ M respectively for donor 1 and close to 1.2 μ M and 1.6 μ M respectively for donor 2 (Figure 4, left). No EC₅₀ could be determined for both compounds on resting human PBMC due to the plateau shaped dose-response curves (Figure 4, right). Human cancer cell lines showed higher sensitivity in terms of EC₅₀ to **6z** than human PBMC indicating that even if **6z** might induce immunosuppression in clinic, this should be manageable and there could be a therapeutic window for **6z** in a broad range of cancer types. Nevertheless, these results suggest that a

1
2
3
4
5
6
7
8
9
10
11
12
13
14
15
16
17
18
19
20
21
22
23
24
25
26
27
28
29
30
31
32
33
34
35
36
37
38
39
40
41
42
43
44
45
46
47
48
49
50
51
52
53
54
55
56
57
58
59
60

compound optimization stage, most probably by re-designing **6z** to selectively avoid inhibition of LCK, could still improve its safety profile to prevent potential side effects and immunosuppressive complications.¹⁹

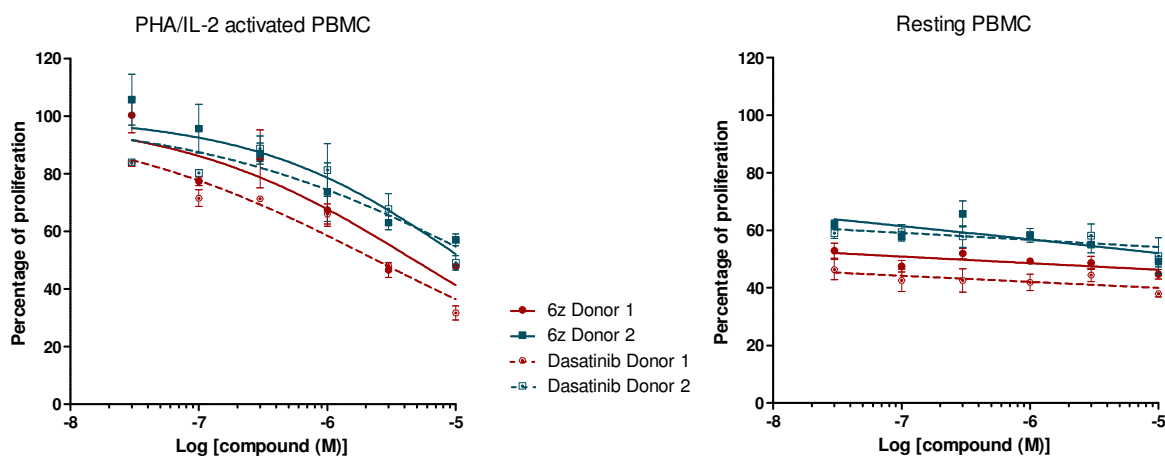


Figure 4. *in vitro* evaluation of cytotoxic effect of **6z** on activated (PHA/IL-2) or resting human PBMC from 2 healthy donors (error bars represent SD).

CONCLUSIONS

Using structure-based drug design combined with medicinal chemistry approaches, we have designed and synthesized a new and potent 7-azaindole-based chemical series showing a multi-target kinase inhibition profile. The compounds from the new series are all type-II inhibitors and are follow-up series from the study of dual ABL and SRC kinase type-I inhibitors we published previously.⁸

A library of more than forty type-II kinase inhibitors was synthesized in 3 to 6 chemical steps from commercially available 7-azaindole scaffolds.

A step wise medicinal chemistry was used to perform pharmacomodulations around the 7-azaindole core and to increase the potency of compounds to obtain a multi-target kinase

1
2
3 inhibition profile against six main targets. The selected targets are representative kinases from
4
5 the growth receptor tyrosine kinase family, the SRC family with c-SRC, and B-RAF kinase as
6
7 one of the first kinases involved in the MAPK signaling pathway activation.
8
9

10 This study highlights the importance of the substitutions in the 7-azaindole core for modulating
11
12 the activity of the compounds on the kinases of interest. Depending on the nature of the
13
14 substituents, we were able to design multi-target kinase inhibitors with different inhibition
15
16 profiles. The study also resulted in the design of a new lead series showing a broad anti-
17
18 proliferative effect on solid and liquid tumors and outperforming the reference compounds for
19
20 the therapeutic indication of interest. The compounds also showed more potent anti-angiogenic
21
22 activity than Sorafenib whose anti-angiogenic activity is considered to be a driver of its anti-
23
24 cancer action.
25
26
27
28

29 All these studies allowed us to select the compound **6z** as our lead for further *in silico* and *in*
30
31 *vitro* investigations. The study of the binding mode of the lead compound **6z** in docking studies
32
33 revealed similar interaction modes for all the six targets (Figures S1 and S2 in supporting
34
35 information document), which explains the MTKI profile. The lead compound also showed very
36
37 good potency on other oncogenic kinases and no inhibition of kinases leading to moderate to
38
39 severe side effects. In anti-proliferation cell assays and compared to several reference and
40
41 marketed anticancer drugs for resistant and wild type cancer indications (hepatocarcinoma, non-
42
43 small cell lung cancer, pancreas, kidney, leukemia, breast), **6z** showed high cytotoxicity with
44
45 potency similar to or even higher than reference compounds. In preliminary ADME-Tox studies,
46
47 **6z** was not predicted to induce potentially cardiotoxic side-effects and presented a favorable
48
49 pharmacokinetic profile in mice. Nevertheless, the compound might potentially induce
50
51 immunosuppression, as number of other kinase inhibitors that should be manageable in clinic. To
52
53
54
55
56
57
58
59
60

1
2
3 conclude, the **6z** lead compound is a highly potent inhibitor with a broad oncogenic kinase
4 spectrum and provides a strong rationale for its therapeutic application in multiple cancer
5 models. However, a lead optimization phase should be started in order to improve its safety
6 profile and prevent potential immunosuppressive complications.
7
8
9
10
11

12 13 14 15 **EXPERIMENTAL SECTION**

16 17 **Chemistry**

18
19 Starting materials, reagents and solvents employed for reactions were reagent grade and used
20 as purchased. Flash column chromatography was performed using either irregular 40-63 μm
21 silica gel or KP-C18-HS Biotage SnapCartridge for the reverse phase. $^1\text{H-NMR}$ spectra were
22 recorded on Bruker Avance 200, 300 or 400 MHz spectrometers using $\text{DMSO-}d_6$. Chemical
23 shifts are reported in parts per million (δ relative to the residual solvent peak). The multiplicity
24 of the signals is indicated with the following abbreviations: bs (broad singlet), s (singlet), d
25 (doublet), t (triplet), q (quartet), m (multiplet), bs (broad singlet), dd (doublet of doublets), td
26 (doublet of triplets). Reaction monitoring and compound purity were determined by LC/MS
27 using Agilent technology 1260 Infinity HPLC system with a C18 column (Agilent ZORBAX
28 SB-C18, 1.8 μm , 2.1 mm x 50 mm) operating at 30°C and coupled with a single quadrupole
29 spectrometer (Agilent 6100). The eluting solvents are: water containing 0.1% formic acid
30 (mobile phase A) and acetonitrile containing 0.1% formic acid (mobile phase B). Three methods
31 were used with 3 different gradient elutions as described in the supporting information section.
32 Detection was carried out with 1) a Diode Array Detector at 254 nm except if specified in the
33 experimental part; and 2) Electrospray Ionization (positive and/or negative mode). The HPLC
34 purity of all final compounds was $\geq 95\%$ except if specified in experimental section.
35
36
37
38
39
40
41
42
43
44
45
46
47
48
49
50
51
52
53
54
55
56
57
58
59
60

1
2
3 **5-(2-methyl-5-nitro-benzylamino)-1*H*-pyrrolo[2,3-*b*]pyridine-2-carboxylic acid methyl ester**
4
5
6 **(3a)**

7
8 5-Amino-1*H*-pyrrolo[2,3-*b*]pyridine-2-carboxylic acid methyl ester **1a** (12.16 g, 63.7 mmol)
9
10 and 2-methyl-5-nitrobenzaldehyde **2** (10.5 g, 64 mmol) were stirred in a solution of AcOH 10%
11
12 in MeOH (660 mL) for 2 h. Then NaBH₃CN (7.9 g, 127 mmol) was slowly added and the
13
14 mixture was stirred under argon for 48 h. Solvents were evaporated and a saturated aqueous
15
16 solution of NaHCO₃ was added until neutrality. Solid formed was filtered and washed with
17
18 petroleum ether/EtOAc 5/5. A brownish solid was obtained (**3a**, 17.9 g, 82%). ¹H-NMR (300
19
20 MHz, DMSO-*d*₆) δ 12.09 (s, 1H), 8.12 (d, *J* = 2.5 Hz, 2H), 8.04 (dd, *J* = 2.5, 8.3 Hz, 1H), 7.50
21
22 (d, *J* = 8.3 Hz, 1H), 7.00 (d, *J* = 2.6 Hz, 1H), 6.88 (s, 1H), 6.30 (t, *J* = 5.8 Hz, 1H), 4.37 (d, *J* =
23
24 5.8 Hz, 2H), 3.82 (s, 3H), 2.49 (s, 4H). MS (ESI) *m/z* 341.1 [M+H]⁺ and 339.1 [M-H]⁻. HPLC
25
26 purity: 94%.

27
28
29
30
31 **1-[5-(2-Methyl-5-nitro-benzylamino)-1*H*-pyrrolo[2,3-*b*]pyridin-2-yl]-ethanone (3b)**

32
33 1-[5-amino-1*H*-pyrrolo[2,3-*b*]pyridin-2-yl]-ethanone **3b** (6.7 g, 0.038 mol) and 2-methyl-5-
34
35 nitrobenzaldehyde **2** (6.3 g, 0.038 mol) were stirred in AcOH/MeOH (42 mL/420mL) for 2 h at
36
37 room temperature. Then NaBH₃CN (4.8 g, 0.076 mol) was slowly added and the mixture was
38
39 stirred under argon overnight. Solvents were evaporated and a saturated aqueous solution of
40
41 NaHCO₃ was added until neutrality. Solid formed was filtered and washed with water and
42
43 diethylether to give the **3b** (10.5g, 86%). ¹H-NMR (300 MHz, DMSO-*d*₆) δ 11.88 (s, 1H), 8.18 –
44
45 8.09 (m, 2H), 8.04 (dd, *J* = 8.3, 2.5 Hz, 1H), 7.51 (d, *J* = 8.3 Hz, 1H), 7.05 (d, *J* = 1.9 Hz, 1H),
46
47 7.00 (d, *J* = 2.5 Hz, 1H), 6.32 (t, *J* = 5.7 Hz, 1H), 4.38 (d, *J* = 5.7 Hz, 2H), 2.49 (s, 3H), 2.47 (s,
48
49 3H). MS (ESI) *m/z* 325.1 [M+H]⁺ and 323.2 [M-H]⁻.

1
2
3 **5-(5-amino-2-methyl-benzylamino)-1H-pyrrolo[2,3-*b*]pyridine-2-carboxylic acid methyl**
4 **ester (4a)**
5
6

7
8 5-(2-Methyl-5-nitro-benzylamino)-1H-pyrrolo[2,3-*b*]pyridine-2-carboxylic acid methyl ester
9
10 **3a** (17.8 g, 54 mmol), methanol (300 mL), 7.2 mL of HCl 12N and palladium 10% on charcoal
11 (1.7 g, 10% w/w) were put in an autoclave filled with 30 bar of hydrogen and stirred for 48 h at
12 room temperature. The mixture was filtered on celite bed and washed with methanol. Solvent
13 was evaporated, and then a saturated aqueous solution of NaHCO₃ was added. The solid obtained
14 was filtered and washed with water to obtain a brownish solid (**4a**, 14.4 g, 96%). ¹H-NMR (300
15 MHz, DMSO-*d*₆) δ 12.02 (s, 1H), 8.07 (d, *J* = 2.6 Hz, 1H), 6.95 (d, *J* = 2.6 Hz, 1H), 6.89 (d, *J* =
16 2.1 Hz, 1H), 6.83 (d, *J* = 8.0 Hz, 1H), 6.58 (d, *J* = 2.3 Hz, 1H), 6.37 (dd, *J* = 8.0, 2.3 Hz, 1H),
17 5.96 – 5.88 (m, 1H), 4.82 (s, 2H), 4.07 (d, *J* = 3.6 Hz, 2H), 3.83 (s, 3H), 2.16 (s, 3H). MS (ESI)
18 *m/z* 311.2 [M+H]⁺.
19
20
21
22
23
24
25
26
27
28
29
30
31

32 **1-[5-(5-amino-2-methyl-benzylamino)-1H-pyrrolo[2,3-*b*]pyridin-2-yl]-ethanone (4b)**
33

34 In an autoclave, 1-[5-(2-methyl-5-nitro-benzylamino)-1H-pyrrolo[2,3-*b*]pyridin-2-yl]-ethanone
35 **3b** (10.7 g, 0.033 mol) and Pd/C 10% (20% w/w, 2 g) in 400 mL DMF were stirred at room
36 temperature under hydrogen pressure (30 bars). After full conversion, the mixture was filtered on
37 a pad of celite and washed several times with a solution of MeOH/10% HCl_{aq}. Then the filtrate
38 was neutralized with NaHCO₃ until pH 7-8 and the solid formed was filtered and washed with
39 water and diethylether to give the **4b** (9.4 g, 97%). ¹H-NMR (300 MHz, DMSO-*d*₆) δ 11.8 (s,
40 1H), 8.09 (s, 1H), 7.06 (d, *J* = 1.9 Hz, 1H), 6.96 (d, *J* = 2.3 Hz, 1H), 6.83 (d, *J* = 8.0 Hz, 1H),
41 6.58 (d, *J* = 1.9 Hz, 1H), 6.37 (dd, *J* = 8.0, 2.3 Hz, 1H), 5.93 (t, *J* = 5.2 Hz, 1H), 4.77 (s, 2H),
42 4.08 (d, *J* = 5.2 Hz, 2H), 2.48 (s, 3H), 2.17 (s, 3H). MS (ESI) *m/z* 295.2 [M+H]⁺.
43
44
45
46
47
48
49
50
51
52
53
54
55
56
57
58
59
60

1
2
3 **Preparation of 5-{2-methyl-5-[3-amido]-benzylamino}-1*H*-pyrrolo[2,3-*b*]pyridine-2-**
4 **carboxylic methyl esters (Compounds 6)**
5
6

7
8 **- General procedure A from carboxylic acids**
9

10 Acid derivative was dissolved in anhydrous DMF with DIEA and HATU or PyBOP. After 15
11 min, compound **4a** or **4b** was slowly added and the mixture was stirred overnight at room
12 temperature. DMF was evaporated and saturated NaHCO₃ aqueous solution was added. The
13 crude mixture was extracted with EtOAc, dried over Na₂SO₄, filtered and evaporated to obtain a
14 dark mixture. After purification by washing with MeOH or by purification on flash
15 chromatography column, expected product was obtained as a slightly yellow or orange powder.
16
17
18
19
20
21
22
23

24 **- General procedure B from acyl chlorides**
25

26 Triethylamine and acyl chloride were added to a solution of compound **4a** or **4b** in anhydrous
27 DMF. The reaction mixture was stirred overnight at room temperature. DMF was evaporated and
28 saturated NaHCO₃ aqueous solution was added. The crude was extracted with EtOAc, dried over
29 Na₂SO₄, filtered and evaporated to obtain a dark mixture. After purification by washing with
30 MeOH or EtOAc or by purification on silica gel column, expected product is obtained as a
31 slightly yellow or orange powder.
32
33
34
35
36
37
38
39
40

41 **5-[2-Methyl-5-(3-methyl-benzoylamino)-benzylamino]-1*H*-pyrrolo[2,3-*b*]pyridine-2-**
42 **carboxylic acid methyl ester (6a)**
43
44

45 The reaction was carried out as described in general procedure A using **4a** (50 mg, 0.16 mmol),
46 3-methylbenzoic acid (22 mg, 0.16 mmol), HATU (182 mg, 0.48 mmol), DIEA (140 μL, 0.8
47 mmol) and anhydrous DMF (3 mL). Purification by reverse phase flash chromatography
48 (H₂O/ACN, 70/30 to 20/80) yielded **6a** (20 mg, 29%). ¹H-NMR (400 MHz, DMSO-*d*₆) δ 12.04
49 (s, 1H), 10.11 (s, 1H), 8.09 (d, *J* = 2.5 Hz, 1H), 7.77 – 7.59 (m, 4H), 7.38 – 7.33 (m, 2H), 7.17
50 (s, 1H), 10.11 (s, 1H), 8.09 (d, *J* = 2.5 Hz, 1H), 7.77 – 7.59 (m, 4H), 7.38 – 7.33 (m, 2H), 7.17
51 (s, 1H), 10.11 (s, 1H), 8.09 (d, *J* = 2.5 Hz, 1H), 7.77 – 7.59 (m, 4H), 7.38 – 7.33 (m, 2H), 7.17
52 (s, 1H), 10.11 (s, 1H), 8.09 (d, *J* = 2.5 Hz, 1H), 7.77 – 7.59 (m, 4H), 7.38 – 7.33 (m, 2H), 7.17
53 (s, 1H), 10.11 (s, 1H), 8.09 (d, *J* = 2.5 Hz, 1H), 7.77 – 7.59 (m, 4H), 7.38 – 7.33 (m, 2H), 7.17
54 (s, 1H), 10.11 (s, 1H), 8.09 (d, *J* = 2.5 Hz, 1H), 7.77 – 7.59 (m, 4H), 7.38 – 7.33 (m, 2H), 7.17
55 (s, 1H), 10.11 (s, 1H), 8.09 (d, *J* = 2.5 Hz, 1H), 7.77 – 7.59 (m, 4H), 7.38 – 7.33 (m, 2H), 7.17
56 (s, 1H), 10.11 (s, 1H), 8.09 (d, *J* = 2.5 Hz, 1H), 7.77 – 7.59 (m, 4H), 7.38 – 7.33 (m, 2H), 7.17
57 (s, 1H), 10.11 (s, 1H), 8.09 (d, *J* = 2.5 Hz, 1H), 7.77 – 7.59 (m, 4H), 7.38 – 7.33 (m, 2H), 7.17
58 (s, 1H), 10.11 (s, 1H), 8.09 (d, *J* = 2.5 Hz, 1H), 7.77 – 7.59 (m, 4H), 7.38 – 7.33 (m, 2H), 7.17
59 (s, 1H), 10.11 (s, 1H), 8.09 (d, *J* = 2.5 Hz, 1H), 7.77 – 7.59 (m, 4H), 7.38 – 7.33 (m, 2H), 7.17
60 (s, 1H), 10.11 (s, 1H), 8.09 (d, *J* = 2.5 Hz, 1H), 7.77 – 7.59 (m, 4H), 7.38 – 7.33 (m, 2H), 7.17

(d, $J = 8.2$ Hz, 1H), 6.98 (s, $J = 2.5$ Hz, 1H), 6.90 (d, $J = 2.1$ Hz, 1H), 6.05 (t, $J = 5.2$ Hz, 1H), 4.21 (d, $J = 5.2$ Hz, 2H), 3.82 (s, 3H), 2.36 (s, 3H), 2.32 (s, 3H). MS (ESI) m/z 429.2 [M+H]⁺ and 427.2 [M-H]⁻. HPLC purity: 93%.

5-[5-(3-Bromo-benzoylamino)-2-methyl-benzylamino]-1H-pyrrolo[2,3-*b*]pyridine-2-carboxylic acid methyl ester (6b)

The reaction was carried out as described in general procedure A using **4a** (150 mg, 0.48 mmol), 3-bromobenzoic acid (96 mg, 0.48 mmol), HATU (500 mg, 1.3 mmol), DIEA (420 μ L, 2.42 mmol) and anhydrous DMF (10 mL). Purification by reverse phase flash chromatography (H₂O/ACN, 75/25 to 25/75) yielded **6b** (57 mg, 24%). ¹H-NMR (400 MHz, DMSO-*d*₆) δ 10.25 (s, 1H), 8.14 – 8.06 (m, 2H), 7.92 – 7.87 (m, 1H), 7.78 – 7.73 (m, 1H), 7.70 – 7.62 (m, 2H), 7.45 (t, $J = 7.9$ Hz, 1H), 7.18 (d, $J = 7.9$ Hz, 1H), 6.98 (d, $J = 2.6$ Hz, 1H), 6.90 (d, $J = 2.1$ Hz, 1H), 6.07 (t, $J = 5.4$ Hz, 1H), 4.22 (d, $J = 5.4$ Hz, 2H), 3.82 (s, 3H), 2.32 (s, 3H). MS (ESI) m/z 493.1-495.1 [M+H]⁺ and 491.1-493.1 [M-H]⁻. HPLC purity: 83% at 295 nm.

5-[5-(3-Isopropyl-benzoylamino)-2-methyl-benzylamino]-1H-pyrrolo[2,3-*b*]pyridine-2-carboxylic acid methyl ester (6c)

The reaction was carried out as described in general procedure A using **4a** (50 mg, 0.16 mmol), 3-Isopropylbenzoic acid (26 mg, 0.16 mmol), HATU (182 mg, 0.48 mmol), DIEA (140 μ L, 0.8 mmol) and anhydrous DMF (3 mL). Purification by reverse phase flash chromatography (H₂O/ACN, 75/25 to 0/100) yielded **6c** (19 mg, 26%). ¹H-NMR (600 MHz, DMSO-*d*₆) δ 12.00 (s, 1H), 10.08 (s, 1H), 8.10 (d, $J = 2.4$ Hz, 1H), 7.76 (s, 1H), 7.71 (d, $J = 7.6$ Hz, 1H), 7.69 (s, 1H), 7.64 (dd, $J = 8.2, 1.8$ Hz, 1H), 7.43 (t, $J = 7.6$ Hz, 1H), 7.39 (t, $J = 7.6$ Hz, 1H), 7.17 (d, $J = 8.2$ Hz, 1H), 7.00 (d, $J = 2.4$ Hz, 1H), 6.90 (d, $J = 1.8$ Hz, 1H), 6.00 (t, $J = 5.4$ Hz, 1H), 4.22

(d, $J = 5.4$ Hz, 2H), 3.83 (s, 3H), 2.99 – 2.93 (q, $J = 7.0$ Hz, 1H), 2.33 (s, 3H), 1.23 (d, $J = 7.0$ Hz, 6H). MS (ESI) m/z 457.3 $[M+H]^+$ and 455.2 $[M-H]^-$. HPLC purity: 94%.

5-[2-Methyl-5-(3-trifluoromethyl-benzoylamino)-benzylamino]-1H-pyrrolo[2,3-*b*]pyridine-2-carboxylic acid methyl ester (6d)

The reaction was carried out as described in general procedure A using **4a** (100 mg, 0.32 mmol), 3-trifluoromethylbenzoic acid (72.2 mg, 0.38 mmol), HATU (145.9 mg, 0.38 mmol), DIEA (220 μ L, 1.26 mmol) and anhydrous DMF (4 mL). Purification by reverse phase flash chromatography (H_2O/ACN with 1% TFA, 100/0 to 30/70) yielded after neutralization with $NaHCO_{3(aq)}$ and filtration **6d** (37 mg, 24%). 1H -NMR (400 MHz, $DMSO-d_6$) δ 12.03 (s, 1H), 10.38 (s, 1H), 8.25 – 8.19 (m, 2H), 8.10 (d, $J = 2.7$ Hz, 1H), 7.93 (d, $J = 8.0$ Hz, 1H), 7.74 (t, $J = 8.0$ Hz, 1H), 7.69 – 7.64 (m, 2H), 7.20 (d, $J = 8.0$ Hz, 1H), 6.98 (d, $J = 2.7$ Hz, 1H), 6.91 – 6.88 (m, 1H), 6.07 (t, $J = 5.5$ Hz, 1H), 4.23 (d, $J = 5.5$ Hz, 2H), 3.82 (s, 3H), 2.33 (s, 3H). MS (ESI) m/z 483.2 $[M+H]^+$.

5-[2-Methyl-5-(3-trifluoromethoxy-benzoylamino)-benzylamino]-1H-pyrrolo[2,3-*b*]pyridine-2-carboxylic acid methyl ester (6e)

The reaction was carried out as described in general procedure A using **4a** (50 mg, 0.16 mmol), 3-(trifluoromethoxy)benzoic acid (33 mg, 0.16 mmol), HATU (185 mg, 0.48 mmol), DIEA (140 μ L, 0.8 mmol) and anhydrous DMF (3 mL). Purification by reverse phase flash chromatography (H_2O/ACN , 80/20 to 30/70) yielded **6e** (20 mg, 25%). 1H -NMR (400 MHz, $DMSO-d_6$) δ 12.04 (s, 1H), 10.30 (s, 1H), 8.09 (d, $J = 2.6$ Hz, 1H), 7.98 – 7.94 (m, 1H), 7.87 – 7.84 (m, 1H), 7.70 – 7.61 (m, 3H), 7.60 – 7.55 (m, 1H), 7.19 (d, $J = 8.2$ Hz, 1H), 6.97 (d, $J = 2.5$ Hz, 1H), 6.89 (d, $J = 2.1$ Hz, 1H), 6.08 (t, $J = 5.3$ Hz, 1H), 4.22 (d, $J = 5.3$ Hz, 2H), 3.82 (s, 3H), 2.33 (s, 3H). MS (ESI) m/z 499.2 $[M+H]^+$ and 497.2 $[M-H]^-$. HPLC purity: 94%.

1
2
3 **5-[2-Methyl-5-(4-methyl-3-trifluoromethyl-benzoylamino)-benzylamino]-1H-pyrrolo[2,3-**
4
5
6 **b]pyridine-2-carboxylic acid methyl ester (6f)**

7
8 The reaction was carried out as described in general procedure A using **4a** (100 mg, 0.32 mmol),
9
10 4-methyl-3-(trifluoromethyl)benzoic acid (73 mg, 0.36 mmol), HATU (147 mg, 0.38 mmol),
11
12 DIEA (167 μ L, 0.96 mmol) and anhydrous DMF (2 mL). Purification by reverse phase flash
13
14 chromatography (H₂O/ACN with 1% TFA, 100/0 to 30/70) yielded after neutralization with
15
16 NaHCO_{3(aq)} and filtration **6f** (41 mg, 26%). ¹H-NMR (300 MHz, DMSO-*d*₆) δ 12.10 (s, 1H),
17
18 10.32 (s, 1H), 8.19 (s, 1H), 8.15 – 8.03 (m, 2H), 7.72 – 7.61 (m, 2H), 7.58 (d, *J* = 8.1 Hz, 1H),
19
20 7.19 (d, *J* = 8.1 Hz, 1H), 7.05 (s, 1H), 6.92 (s, 1H), 4.24 (s, 2H), 3.83 (s, 3H), 2.50 (s, 3H), 2.32
21
22 (s, 3H). MS (ESI) *m/z* 497.2 [M+H]⁺ and 495.1 [M-H]⁻.
23
24
25
26

27 **5-[5-(4-Chloro-3-trifluoromethyl-benzoylamino)-2-methyl-benzylamino]-1H-pyrrolo[2,3-**
28
29 **b]pyridine-2-carboxylic acid methyl ester (6g)**

30
31 The reaction was carried out as described in general procedure A using **4a** (100 mg, 0.32 mmol),
32
33 4-chloro-3-(trifluoromethyl)benzoic acid (80 mg, 0.36 mmol), HATU (147 mg, 0.35 mmol),
34
35 DIEA (167 μ L, 0.96 mmol) and anhydrous DMF (2 mL). Purification by reverse phase flash
36
37 chromatography (H₂O/ACN with 1% TFA, 100/0 to 40/60) yielded after neutralization with
38
39 NaHCO_{3(aq)} and filtration **6g** (8 mg, 5%). ¹H-NMR (300 MHz, DMSO-*d*₆) δ 12.05 (s, 1H), 10.43
40
41 (s, 1H), 8.33 (s, 1H), 8.21 (d, *J* = 7.9 Hz, 1H), 8.10 (s, 1H), 7.87 (d, *J* = 8.4 Hz, 1H), 7.70 – 7.60
42
43 (m, 2H), 7.20 (d, *J* = 8.4 Hz, 1H), 6.98 (s, 1H), 6.90 (s, 1H), 6.10 (s, 1H), 4.23 (s, 2H), 3.82 (s,
44
45 3H), 2.33 (s, 3H). MS (ESI) *m/z* 517.1 [M+H]⁺ and 515.0 [M-H]⁻.
46
47
48
49
50

51 **5-[5-(4-Hydroxy-3-trifluoromethyl-benzoylamino)-2-methyl-benzylamino]-1H-**
52
53 **pyrrolo[2,3-*b*]pyridine-2-carboxylic acid methyl ester (6h)**
54
55
56
57
58
59
60

1
2
3 The reaction was carried out as described in general procedure A using **4a** (50 mg, 0.16 mmol),
4 4-hydroxy-3-(trifluoromethoxy)benzoic acid (33 mg, 0.16 mmol), HATU (182 mg, 0.48 mmol),
5 DIEA (140 μ L, 0.8 mmol) and anhydrous DMF (3 mL). Purification by reverse phase flash
6 chromatography (H₂O/ACN, 80/20 to 30/70) yielded **6h** (12 mg, 15%). ¹H-NMR (400 MHz,
7 DMSO-*d*₆) δ 12.03 (s, 1H), 10.07 (s, 1H), 8.12 – 8.08 (m, 2H), 8.01 (dd, *J* = 8.8, 1.6 Hz, 1H),
8 7.65 (d, *J* = 2.0 Hz, 1H), 7.63 (dd, *J* = 8.1, 2.0 Hz, 1H), 7.16 (d, *J* = 8.1 Hz, 1H), 7.02 (d, *J* = 8.8
9 Hz, 1H), 7.00 – 6.97 (m, 1H), 6.92 – 6.88 (m, 1H), 6.03 (t, *J* = 5.3 Hz, 1H), 4.21 (d, *J* = 5.3 Hz,
10 2H), 3.82 (s, 3H), 2.32 (s, 3H). MS (ESI) *m/z* 499.2 [M+H]⁺ and 497.1 [M-H]⁻.
11
12
13
14
15
16
17
18
19
20
21
22
23
24

25 **5-[5-(3-Dimethylamino-5-trifluoromethyl-benzoylamino)-2-methyl-benzylamino]-1H-**
26 **pyrrolo[2,3-*b*]pyridine-2-carboxylic acid methyl ester (6i)**
27
28

29 The reaction was carried out as described in general procedure A using **4a** (80 mg, 0.26 mmol),
30 3-dimethylamino-5-(trifluoromethyl)benzoic acid (60 mg, 0.26 mmol), HATU (288 mg, 0.78
31 mmol), DIEA (250 μ L, 1.3 mmol) and anhydrous DMF (4 mL). Purification by reverse phase
32 flash chromatography (H₂O/ACN, 70/30 to 30/70) yielded **6i** (32 mg, 23%). ¹H-NMR (200 MHz,
33 DMSO-*d*₆) δ 12.05 (s, 1H), 10.25 (s, 1H), 8.09 (s, 1H), 7.71 – 7.57 (m, 2H), 7.42 (d, *J* = 6.3 Hz,
34 2H), 7.18 (d, *J* = 8.0 Hz, 1H), 7.03 (s, 1H), 6.98 (s, 1H), 6.89 (s, 1H), 6.06 (t, *J* = 4.0 Hz, 1H),
35 4.22 (d, *J* = 4.0 Hz, 2H), 3.82 (s, 3H), 3.16 (dd, *J* = 5.1, 1.4 Hz, 2H), 3.03 – 2.96 (m, 6H), 2.32
36 (s, 3H). MS (ESI) *m/z* 526.2 [M+H]⁺ and 524.2 [M-H]⁻.
37
38
39
40
41
42
43
44
45
46
47

48 **5-[5-(2-Methoxy-benzoylamino)-2-methyl-benzylamino]-1H-pyrrolo[2,3-*b*]pyridine-2-**
49 **carboxylic acid methyl ester (6j)**
50
51

52 The reaction was carried out as described in general procedure B using **4a** (100 mg, 0.32 mmol),
53 2-methoxybenzoyl chloride (57 μ L, 0.38 mmol), Et₃N (134 μ L, 0.96 mmol) and anhydrous DMF
54
55
56
57
58
59
60

(2 mL). Purification by reverse phase flash chromatography (H₂O/ACN with 1% TFA, 100/0 to 0/100) yielded after neutralization with NaHCO_{3(aq)} and filtration **6j** (34.5 mg, 24%). ¹H-NMR (300 MHz, DMSO-*d*₆) δ 12.03 (s, 1H), 10.00 (s, 1H), 8.09 (d, *J* = 2.0 Hz, 1H), 7.73 – 7.55 (m, 3H), 7.50 – 7.42 (m, 1H), 7.15 (t, *J* = 7.7 Hz, 2H), 7.09 – 6.97 (m, 2H), 6.90 (d, *J* = 2.0 Hz, 1H), 6.01 (t, *J* = 5.0 Hz, 1H), 4.20 (d, *J* = 5.0 Hz, 2H), 3.83 (s, 3H), 3.83 (s, 3H), 2.31 (s, 3H). MS (ESI) *m/z* 445.2 [M+H]⁺ and 443.2 [M-H]⁻.

5-{5-[2-(2-Bromo-phenyl)-acetylamino]-2-methyl-benzylamino}-1H-pyrrolo[2,3-*b*]pyridine-2-carboxylic acid methyl ester (6k)

The reaction was carried out as described in general procedure B using **4a** (20 mg, 0.065 mmol), 2-bromophenylacetyl chloride (10 μL, 0.065 mmol), Et₃N (18 μL, 0.13 mmol) and anhydrous DMF (2 mL). Purification by reverse phase flash chromatography (H₂O/ACN, 80/20 to 20/80) yielded **6k** (7 mg, 11%). ¹H-NMR (400 MHz, DMSO-*d*₆) δ 12.02 (s, 1H), 10.06 (s, 1H), 8.08 (d, *J* = 2.6 Hz, 1H), 7.65 – 7.49 (m, 1H), 7.42 (s, 1H), 7.39 – 7.29 (m, 2H), 7.22 – 7.15 (m, 1H), 7.11 (d, *J* = 8.1 Hz, 1H), 6.96 – 6.91 (m, 1H), 6.89 (s, 1H), 6.08 – 6.01 (m, 1H), 4.23 – 4.14 (m, 2H), 3.83 (s, 3H), 3.76 (s, 2H), 2.28 (s, 3H). MS (ESI) *m/z* 505.1, 507.1[M+H]⁺.

5-{2-Methyl-5-[2-(3-trifluoromethyl-phenyl)-acetylamino]-benzylamino}-1H-pyrrolo[2,3-*b*]pyridine-2-carboxylic acid methyl ester (6l)

The reaction was carried out as described in general procedure A using **4a** (50 mg, 0.16 mmol), 3-(trifluoromethyl)phenylacetic acid (33 mg, 0.16 mmol), HATU (180 mg, 0.48 mmol), DIEA (140 μL, 0.8 mmol) and anhydrous DMF (3 mL). Purification by reverse phase flash chromatography (H₂O/ACN, 85/15 to 0/100) yielded **6l** (9 mg, 11%). ¹H-NMR (600 MHz, DMSO-*d*₆) δ 12.00 (s, 1H), 10.07 (s, 1H), 8.08 (d, *J* = 2.5 Hz, 1H), 7.64 (s, 1H), 7.61 – 7.56 (m,

1
2
3 2H), 7.56 – 7.51 (m, 2H), 7.43 (s, 1H), 7.11 (d, $J = 8.2$ Hz, 1H), 6.95 (d, $J = 2.4$ Hz, 1H), 6.88
4
5 (d, $J = 1.1$ Hz, 1H), 6.02 (t, $J = 5.5$ Hz, 1H), 4.19 (d, $J = 5.5$ Hz, 2H), 3.83 (s, 3H), 3.70 (s, 2H),
6
7 2.28 (s, 3H). MS (ESI) m/z 497.2 $[M+H]^+$ and 495.2 $[M-H]^-$. HPLC purity: 94%.

10
11 **5-{2-Methyl-5-[(5-methyl-pyridine-3-carbonyl)-amino]-benzylamino}-1H-pyrrolo[2,3-**
12
13 **b]pyridine-2-carboxylic acid methyl ester (6m)**

14
15 The reaction was carried out as described in general procedure A using **4a** (100 mg, 0.32 mmol),
16
17 5-methylnicotinic acid (50.9 mg, 0.37 mmol), HATU (146 mg, 0.38 mmol), DIEA (220 μ L, 1.28
18
19 mmol) and anhydrous DMF (4 mL). Purification by reverse phase flash chromatography
20
21 (H₂O/ACN with 1% TFA, 100/0 to 30/70) yielded after neutralization with NaHCO_{3(aq)} and
22
23 filtration **6m** (28 mg, 20%). ¹H-NMR (300 MHz, DMSO-*d*₆) δ 12.04 (s, 1H), 10.29 (s, 1H), 8.85
24
25 (s, 1H), 8.55 (s, 1H), 8.20 – 7.95 (m, 2H), 7.85 – 7.55 (m, 2H), 7.21 (s, 1H), 7.04 – 6.82 (m, 2H),
26
27 6.08 (s, 1H), 4.22 (s, 2H), 3.82 (s, 3H), 2.42 – 2.22 (m, 6H). MS (ESI) m/z 430.2 $[M+H]^+$ and
28
29 428.1 $[M-H]^-$. HPLC purity: 94%.

32
33
34 **5-{2-Methyl-5-[(2-methyl-pyridine-4-carbonyl)-amino]-benzylamino}-1H-pyrrolo[2,3-**
35
36 **b]pyridine-2-carboxylic acid methyl ester (6n)**

37
38 The reaction was carried out as described in general procedure A using **4a** (100 mg, 0.32 mmol),
39
40 2-methylisonicotinic acid (52 mg, 0.38 mmol), HATU (146 mg, 0.38 mmol), DIEA (220 μ L,
41
42 1.28 mmol) and anhydrous DMF (4 mL). Purification by reverse phase flash (H₂O/ACN with 1%
43
44 TFA, 100/0 to 30/70) yielded after neutralization with NaHCO_{3(aq)} and filtration **6n** (27 mg,
45
46 20%). ¹H-NMR (300 MHz, DMSO-*d*₆) δ 10.34 (s, 1H), 8.58 (d, $J = 4.9$ Hz, 1H), 8.14 – 8.03 (m,
47
48 1H), 7.72 – 7.50 (m, 4H), 7.19 (d, $J = 7.9$ Hz, 1H), 7.00 – 6.92 (m, 1H), 6.89 (s, 1H), 6.08 (t, $J =$
49
50 4.7 Hz, 1H), 4.23 (d, $J = 4.7$ Hz, 2H), 3.82 (s, 3H), 2.53 (s, 3H), 2.33 (s, 3H). MS (ESI) m/z
51
52 430.2 $[M+H]^+$ and 428.2 $[M-H]^-$.

1
2
3 **5-{2-Methyl-5-[(5-trifluoromethyl-pyridine-3-carbonyl)-amino]-benzylamino}-1H-**
4
5
6 **pyrrolo[2,3-*b*]pyridine-2-carboxylic acid methyl ester (6o)**

7
8 The reaction was carried out as described in general procedure A using **4a** (50 mg, 0.16 mmol),
9
10 nicotinic acid (31 mg, 0.16 mmol), HATU (180 mg, 0.48 mmol), DIEA (150 μ L, 0.8 mmol) and
11
12 anhydrous DMF (3 mL). Purification by reverse phase flash chromatography (H₂O /ACN, 80/20
13
14 to 30/70) yielded **6o** (10 mg, 13%). ¹H-NMR (400 MHz, DMSO-*d*₆) δ 12.02 (s, 1H), 10.52 (s,
15
16 1H), 9.31 (s, 1H), 9.14 (s, 1H), 8.62 (s, 1H), 8.09 (d, *J* = 2.5 Hz, 1H), 7.71 – 7.63 (m, 2H), 7.22
17
18 (d, *J* = 8.9 Hz, 1H), 6.96 (d, *J* = 2.4 Hz, 1H), 6.89 (d, *J* = 2.0 Hz, 1H), 6.10 (t, *J* = 5.4 Hz, 1H),
19
20 4.24 (d, *J* = 5.4 Hz, 2H), 3.82 (s, 3H), 2.34 (s, 3H). MS (ESI) *m/z* 484.2 [M+H]⁺ and 482.2 [M-
21
22 H]⁻.
23
24
25

26
27 **5-{2-Methyl-5-[(2-trifluoromethyl-pyridine-4-carbonyl)-amino]-benzylamino}-1H-**
28
29 **pyrrolo[2,3-*b*]pyridine-2-carboxylic acid methyl ester (6p)**

30
31 The reaction was carried out as described in general procedure A using **4a** (100 mg, 0.32 mmol),
32
33 2-(trifluoromethyl)pyridine-4-carboxylic acid (73.3 mg, 0.38 mmol), HATU (146 mg, 0.38
34
35 mmol), DIEA (220 μ L, 1.28 mmol) and anhydrous DMF (4 mL). Purification by reverse phase
36
37 flash chromatography (H₂O/ACN with 1% TFA, 100/0 to 40/60) yielded after neutralization with
38
39 NaHCO_{3(aq)} and filtration **6p** (9 mg, 6%). ¹H-NMR (300 MHz, DMSO-*d*₆) δ 12.06 (s, 1H), 10.59
40
41 (s, 1H), 8.94 (d, *J* = 5.6 Hz, 1H), 8.30 (s, 1H), 8.11 (d, *J* = 8.4 Hz, 2H), 7.74 – 7.64 (m, 2H), 7.22
42
43 (d, *J* = 8.4 Hz, 1H), 6.99 (s, 1H), 6.90 (s, 1H), 4.25 (s, 2H), 3.82 (s, 3H), 2.34 (s, 3H). MS (ESI)
44
45 *m/z* 484.1 [M+H]⁺.
46
47
48
49

50
51 **5-{2-Methyl-5-[(6-trifluoromethyl-pyridine-3-carbonyl)-amino]-benzylamino}-1H-**
52
53 **pyrrolo[2,3-*b*]pyridine-2-carboxylic acid methyl ester (6q)**

1
2
3 The reaction was carried out as described in general procedure A using **4a** (100 mg, 0.32 mmol),
4 6-trifluoromethylnicotinic acid (73.3 mg, 0.38 mmol), HATU (146 mg, 0.38 mmol), DIEA (220
5 μL , 1.28 mmol) and anhydrous DMF (4 mL). Purification by reverse phase flash
6 chromatography ($\text{H}_2\text{O}/\text{ACN}$ with 1% TFA, 100/0 to 40/60) yielded after neutralization with
7 $\text{NaHCO}_3(\text{aq})$ and filtration **6q** (23 mg, 14%). $^1\text{H-NMR}$ (300 MHz, $\text{DMSO-}d_6$) δ 12.05 (s, 1H),
8 10.53 (s, 1H), 9.18 (s, 1H), 8.50 (d, $J = 8.0$ Hz, 1H), 8.15 – 8.00 (m, 2H), 7.72 – 7.62 (m, 2H),
9 7.21 (d, $J = 8.0$ Hz, 1H), 7.02 - 6.95 (m, 1H), 6.94 – 6.86 (m, 1H), 4.25 (s, 2H), 3.82 (s, 3H),
10 2.34 (s, 3H). MS (ESI) m/z 484.1 $[\text{M}+\text{H}]^+$ and 482.2 $[\text{M}-\text{H}]^-$.

11
12
13
14
15
16
17
18
19
20
21
22
23
24
25
26
27
28
29
30
31
32
33
34
35
36
37
38
39
40
41
42
43
44
45
46
47
48
49
50
51
52
53
54
55
56
57
58
59
60

5-{5-[(2,3-Dihydro-benzofuran-7-carbonyl)-amino]-2-methyl-benzylamino}-1H-pyrrolo[2,3-*b*]pyridine-2-carboxylic acid methyl ester (6r**)**

The reaction was carried out as described in general procedure B using **4a** (40 mg, 0.13 mmol),
2,3-dihydro-1-benzofuran-7-carbonyl chloride (24 mg, 0.13 mmol), Et_3N (36 μL , 0.26 mmol)
and anhydrous DMF (3 mL). Purification by reverse phase flash chromatography ($\text{H}_2\text{O}/\text{ACN}$,
80/20 to 20/80) yielded **6r** (8 mg, 13%). $^1\text{H-NMR}$ (400 MHz, $\text{DMSO-}d_6$) δ 9.63 (s, 1H), 8.10 (d,
 $J = 2.5$ Hz, 1H), 7.63 (d, $J = 1.8$ Hz, 1H), 7.60 – 7.54 (m, 2H), 7.42 (d, $J = 6.3$ Hz, 1H), 7.18 (d,
 $J = 8.2$ Hz, 1H), 7.02 (d, $J = 2.5$ Hz, 1H), 6.95 (t, $J = 7.6$ Hz, 1H), 6.90 (d, $J = 1.8$ Hz, 1H), 6.00
(t, $J = 5.5$ Hz, 1H), 4.71 (t, $J = 8.7$ Hz, 2H), 4.21 (d, $J = 5.5$ Hz, 2H), 3.82 (s, 3H), 3.24 (t, $J = 8.7$
Hz, 2H), 2.33 (s, 3H). MS (ESI) m/z 457.0 $[\text{M}+\text{H}]^+$ and 455.1 $[\text{M}-\text{H}]^-$. HPLC purity: 90%.

5-{5-[(Benzo[1,3]dioxole-5-carbonyl)-amino]-2-methyl-benzylamino}-1H-pyrrolo[2,3-*b*]pyridine-2-carboxylic acid methyl ester (6s**)**

The reaction was carried out as described in general procedure A using **4a** (31 mg, 0.1 mmol),
1,3- benzodioxole-5-carboxylic acid (17 mg, 0.1 mmol), HATU (115 mg, 0.3 mmol), DIEA (90
 μL , 0.7 mmol) and anhydrous DMF (2 mL). Purification by reverse phase flash chromatography

1
2
3 (H₂O/ACN, 80/20 to 0/100) yielded **6s** (5 mg, 10%). ¹H-NMR (600 MHz, DMSO-*d*₆) δ 12.01 (s,
4 1H), 9.95 (s, 1H), 8.09 (d, *J* = 1.8 Hz, 1H), 7.68 (s, 1H), 7.62 (d, *J* = 8.1 Hz, 1H), 7.53 (d, *J* = 8.4
5 Hz, 1H), 7.47 (s, 1H), 7.16 (d, *J* = 8.1 Hz, 1H), 7.00 (d, *J* = 8.8 Hz, 2H), 6.90 (s, 1H), 6.10 (s,
6 2H), 6.01 (t, *J* = 4.7 Hz, 1H), 4.21 (d, *J* = 4.7 Hz, 2H), 3.83 (s, 3H), 2.32 (s, 3H). MS (ESI) *m/z*
7 459.1 [M+H]⁺ and 457.2 [M-H]⁻. HPLC purity: 93%.

14
15 **5-{5-[(3*H*-Benzotriazole-5-carbonyl)-amino]-2-methyl-benzylamino}-1*H*-pyrrolo[2,3-
16 *b*]pyridine-2-carboxylic acid methyl ester (**6t**)**

17
18 The reaction was carried out as described in general procedure A using **4a** (50 mg, 0.16 mmol),
19
20 1*H*-benzotriazole-5-carboxylic acid (26 mg, 0.16 mmol), HATU (182 mg, 0.48 mmol), DIEA
21
22 (140 μL, 0.8 mmol) and anhydrous DMF (3 mL). Purification by reverse phase flash
23
24 chromatography (H₂O/ACN, 80/20 to 30/70) yielded **6t** (10 mg, 14%). ¹H-NMR (600 MHz,
25
26 DMSO-*d*₆) δ 12.03 (s, 1H), 10.26 (s, 1H), 8.52 (s, 1H), 8.11 (d, *J* = 2.7 Hz, 1H), 7.92 – 7.87 (m,
27
28 2H), 7.74 (d, *J* = 2.0 Hz, 1H), 7.69 (dd, *J* = 7.8, 2.0 Hz, 1H), 7.19 (d, *J* = 8.3 Hz, 1H), 7.03 – 6.98
29
30 (m, 1H), 6.93 – 6.87 (m, 1H), 6.05 (t, *J* = 5.3 Hz, 1H), 4.23 (d, *J* = 5.3 Hz, 2H), 3.82 (s, 3H),
31
32 2.33 (s, 3H). MS (ESI) *m/z* 456.2 [M+H]⁺ and 454.2 [M-H]⁻. HPLC purity: 94%.

33
34 **5-{5-[(1*H*-Indole-5-carbonyl)-amino]-2-methyl-benzylamino}-1*H*-pyrrolo[2,3-*b*]pyridine-
35
36 2-carboxylic acid methyl ester (**6u**)**

37
38 The reaction was carried out as described in general procedure A using **4a** (60 mg, 0.19 mmol),
39
40 1*H*-indole-5-carboxylic acid (31 mg, 0.19 mmol), PyBOP (296 mg, 0.57 mmol), DIEA (165 μL,
41
42 0.95 mmol) and anhydrous DMF (4 mL). Purification by reverse phase flash chromatography
43
44 (H₂O/ACN, 80/20 to 40/60) yielded **6u** (38 mg, 44%). ¹H-NMR (200 MHz, DMSO-*d*₆) δ 12.05
45
46 (s, 1H), 11.36 (s, 1H), 10.03 (s, 1H), 8.21 (d, *J* = 1.2 Hz, 1H), 8.11 (d, *J* = 2.6 Hz, 1H), 7.73 (dd,
47
48 *J* = 6.5, 1.7 Hz, 2H), 7.67 (d, *J* = 1.7 Hz, 1H), 7.51 – 7.42 (m, 2H), 7.16 (d, *J* = 8.2 Hz, 1H), 7.00
49
50
51
52
53
54
55
56
57
58
59
60

(d, $J = 2.6$ Hz, 1H), 6.92 (d, $J = 1.2$ Hz, 1H), 6.61 – 6.49 (m, 1H), 6.05 (t, $J = 5.5$ Hz, 1H), 4.21 (t, $J = 5.5$ Hz, 2H), 3.82 (s, 3H), 2.32 (s, 3H). MS (ESI) m/z 454.0 $[M+H]^+$ and 452.0 $[M-H]^-$.

5-{2-Methyl-5-[4-(2-methyl-thiazol-4-yl)-benzoylamino]-benzylamino}-1H-pyrrolo[2,3-b]pyridine-2-carboxylic acid methyl ester (6v)

The reaction was carried out as described in general procedure B using **4a** (40 mg, 0.13 mmol), 4-(2-methyl-thiazol-4-yl)-benzoyl chloride (30 mg, 0.13 mmol), Et₃N (60 μ L, 0.39 mmol) and anhydrous DMF (2 mL). Purification by reverse phase flash chromatography (H₂O/ACN, 80/20 to 20/80) yielded **6v** (24 mg, 36%). ¹H-NMR (400 MHz, DMSO-*d*₆) δ 12.03 (s, 1H), 10.18 (s, 1H), 8.09 (s, 2H), 8.04 (d, $J = 8.4$ Hz, 2H), 7.98 (d, $J = 8.2$ Hz, 2H), 7.71 (s, 1H), 7.67 (d, $J = 8.4$ Hz, 1H), 7.18 (d, $J = 7.6$ Hz, 1H), 6.99 (s, 1H), 6.90 (s, 1H), 6.05 (t, $J = 5.5$ Hz, 1H), 4.23 (d, $J = 5.5$ Hz, 2H), 3.82 (s, 3H), 2.73 (s, 3H), 2.31 (s, 3H). MS (ESI) m/z 512.2 $[M+H]^+$. HPLC purity: 90%.

5-{2-Methyl-5-[(1H-pyrrole-3-carbonyl)-amino]-benzylamino}-1H-pyrrolo[2,3-b]pyridine-2-carboxylic acid methyl ester (6w)

The reaction was carried out as described in general procedure A using **4a** (100 mg, 0.32 mmol), 1H-pyrrole-3-carboxylic acid (43 mg, 0.38 mmol), HATU (147 mg, 0.38 mmol), DIEA (167 μ L, 0.96 mmol) and anhydrous DMF (3 mL). Purification by reverse phase flash chromatography (H₂O/ACN with 1% TFA, 100/0 to 50/50) yielded after neutralization with NaHCO_{3(aq)} and filtration **6w** (72 mg, 55%). ¹H-NMR (300 MHz, DMSO-*d*₆) δ 12.06 (s, 1H), 11.21 (s, 1H), 9.39 (s, 1H), 8.11 (s, 1H), 7.69-7.62 (m, 1H), 7.64 – 7.58 (m, 1H), 7.51-7.43 (m, 1H), 7.12 (d, $J = 7.9$ Hz, 1H), 7.07-6.99 (m, 1H), 6.94-6.88 (m, 1H), 6.80-6.73 (m, 1H), 6.64-6.56 (m, 1H), 6.30-5.75 (m, 1H), 4.20 (s, 2H), 3.83 (s, 3H), 2.30 (s, 3H). MS (ESI) m/z 404.2 $[M+H]^+$ and 402.1 $[M-H]^-$.

1
2
3
4
5
6
7
8
9
10
11
12
13
14
15
16
17
18
19
20
21
22
23
24
25
26

5-{2-Methyl-5-[4-(4-methyl-piperazin-1-ylmethyl)-benzoylamino]-benzylamino}-1H-pyrrolo[2,3-*b*]pyridine-2-carboxylic acid methyl ester (6x)

The reaction was carried out as described in general procedure A using **4a** (1 g, 3.23 mmol), 4-[(4-methyl-1-piperazinyl)methyl]benzoic acid **5x** (0.9 g, 3.87 mmol), HATU (1.47 g, 3.87 mmol), DIEA (1.7 mL, 9.7 mmol) and anhydrous DMF (50 mL). Purification by washing with MeOH yielded **6x** (565 mg, 33%). ¹H-NMR (300 MHz, DMSO-*d*₆) δ 12.04 (s, 1H), 10.11 (s, 1H), 8.09 (s, 1H), 7.91 – 7.78 (m, 2H), 7.73 – 7.60 (m, 2H), 7.39 (d, *J* = 7.9 Hz, 2H), 7.17 (d, *J* = 7.9 Hz, 1H), 6.98 (s, 1H), 6.90 (s, 1H), 6.11 – 6.00 (m, 1H), 4.21 (d, *J* = 3.7 Hz, 2H), 3.82 (s, 3H), 3.49 (s, 2H), 2.43 – 2.21 (m, 11H), 2.13 (s, 3H). MS (ESI) *m/z* 527.3 [M+H]⁺ and 525.2 [M-H]⁻.

27
28
29
30
31
32
33
34
35
36
37
38
39
40
41
42
43
44
45
46
47
48
49
50
51
52

5-{5-[4-(3-Dimethylamino-pyrrolidin-1-ylmethyl)-3-trifluoromethyl-benzoylamino]-2-methyl-benzylamino}-1H-pyrrolo[2,3-*b*]pyridine-2-carboxylic acid methyl ester (6y)

The reaction was carried out as described in general procedure A using **4a** (3.5 g, 11.3 mmol), 4-(3-dimethylamino-pyrrolidin-1-ylmethyl)-3-trifluoromethyl-benzoic acid **5y** (4.3 g, 13.5 mmol), HATU (8.58 g, 22.6 mmol), DIEA (9.8 mL, 56.4 mmol) and anhydrous DMF (50 mL). Purification by reverse phase flash chromatography (H₂O/ACN with 1% TFA, 70/30 to 50/50) yielded after neutralization with NaHCO_{3(aq)} and filtration **6y** (1.9 g, 28%). ¹H-NMR (400 MHz, DMSO-*d*₆) δ 12.04 (s, 1H), 10.35 (s, 1H), 8.20 – 8.14 (m, 2H), 8.09 (d, *J* = 2.6 Hz, 1H), 7.85 (d, *J* = 7.8 Hz, 1H), 7.68 – 7.62 (m, 2H), 7.19 (d, *J* = 8.8 Hz, 1H), 6.97 (d, *J* = 2.6 Hz, 1H), 6.89 (d, *J* = 2.1 Hz, 1H), 6.08 (t, *J* = 5.3 Hz, 1H), 4.23 (d, *J* = 5.3 Hz, 2H), 3.82 (s, 3H), 3.83 – 3.69 (m, 2H), 2.93 – 2.78 (m, 1H), 2.68 – 2.54 (m, 3H), 2.44 – 2.37 (m, 1H), 2.33 (s, 3H), 2.15 (s, 6H), 1.96 – 1.83 (m, 1H), 1.74 – 1.58 (m, 1H). MS (ESI) *m/z* 609.3 [M+H]⁺ and 607.3 [M-H]⁻.

53
54
55
56
57
58
59
60

1
2
3
4
5
6
7
8
9
10
11
12
13
14
15
16
17
18
19
20
21
22
23
24
25
26
27
28
29
30
31
32
33
34
35
36
37
38
39
40
41
42
43
44
45
46
47
48
49
50
51
52
53
54
55
56
57
58
59
60

5-{2-Methyl-5-[3-(4-methyl-imidazol-1-yl)-5-trifluoromethyl-benzoylamino]-benzylamino}-1*H*-pyrrolo[2,3-*b*]pyridine-2-carboxylic acid methyl ester (6z)

The reaction was carried out as described in general procedure A using **4a** (170 mg, 0.63 mmol), 3-(4-methyl-imidazol-1-yl)-5-trifluoromethyl-benzoic acid **5z** (200 mg, 0.63 mmol), HATU (735 mg, 1.93 mmol), DIEA (0.56 mL, 3.22 mmol) and anhydrous DMF (16 mL). Purification by flash chromatography on silica gel (EtOAc/EtOH, 100/0 to 90/10) yielded **6z** (108 mg, 30%). ¹H-NMR (300 MHz, DMSO-*d*₆) δ 12.05 (s, 1H), 10.41 (s, 1H), 8.42 – 8.34 (m, 2H), 8.20 (s, 1H), 8.16 – 8.04 (m, 2H), 7.670 – 7.62 (m, 3H), 7.22 (d, *J* = 8.2 Hz, 1H), 6.97 (d, *J* = 2.3 Hz, 1H), 6.90 (d, *J* = 1.9 Hz, 1H), 6.11 (t, *J* = 5.0 Hz, 1H), 4.25 (d, *J* = 5.0 Hz, 2H), 3.83 (s, 3H), 2.34 (s, 3H), 2.17 (s, 3H). MS (ESI) *m/z* 563.2 [M+H]⁺ and 561.2 [M-H]⁻.

N-{3-[(2-Acetyl-1*H*-pyrrolo[2,3-*b*]pyridin-5-ylamino)-methyl]-4-methyl-phenyl}-4-(4-methyl-piperazin-1-ylmethyl)-benzamide (7x)

The reaction was carried out as described in general procedure A using **4b** (100 mg, 0.34 mmol), 4-[(4-methyl-1-piperazinyl)methyl]benzoic acid **5x** (111 mg, 0.476 mmol), HATU (155 mg, 0.408 mmol), DIEA (177 μL, 1.02 mmol) and anhydrous DMF (2 mL). Purification by reverse phase flash chromatography (H₂O/ACN with 1% TFA, 100/0 to 50/50) yielded after neutralization with NaHCO_{3(aq)} and filtration **7x** (54 mg, 26%). ¹H-NMR (300 MHz, DMSO-*d*₆) δ 11.82 (s, 1H), 10.10 (s, 1H), 8.11 (d, *J* = 2.0, 1H), 7.85 (d, *J* = 7.8 Hz, 2H), 7.75 – 7.60 (m, 2H), 7.39 (d, *J* = 7.9 Hz, 2H), 7.17 (d, *J* = 7.8 Hz, 1H), 7.06 (s, 1H), 6.98 (s, 1H), 6.07 (t, *J* = 5.2 Hz, 1H), 4.22 (d, *J* = 5.2 Hz, 2H), 3.50 (s, 2H), 2.47 (s, 3H), 2.42 – 2.18 (m, 11H), 2.14 (s, 3H). MS (ESI) *m/z* 511.3 [M+H]⁺ and 509.1 [M-H]⁻.

N-{3-[(2-Acetyl-1*H*-pyrrolo[2,3-*b*]pyridin-5-ylamino)-methyl]-4-methyl-phenyl}-4-(3-dimethylamino-pyrrolidin-1-ylmethyl)-3-trifluoromethyl-benzamide (7y)

1
2
3 The reaction was carried out as described in general procedure A using **4b** (100 mg, 0.34 mmol),
4 4-(3-dimethylamino-pyrrolidin-1-ylmethyl)-3-trifluoromethyl-benzoic acid **5y** (107 mg, 0.34
5 mmol), HATU (258 mg, 0.68 mmol), DIEA (442 μ L, 2.54 mmol) and anhydrous DMF (3 mL).
6
7 Purification by reverse phase flash chromatography (H₂O/ACN with 1% TFA, 100/0 to 50/50)
8 yielded after neutralization with NaHCO_{3(aq)} and filtration **7y** (8 mg, 4%). ¹H-NMR (300 MHz,
9 DMSO-*d*₆) δ 11.83 (s, 1H), 10.36 (s, 1H), 8.21 – 8.15 (m, 2H), 8.12 (d, *J* = 2.6 Hz, 1H), 7.85 (d,
10 *J* = 8.6 Hz, 1H), 7.70 – 7.62 (m, 2H), 7.19 (d, *J* = 7.9 Hz, 1H), 7.06 (s, 1H), 6.98 (d, *J* = 2.6 Hz,
11 1H), 6.11 (t, *J* = 5.2 Hz, 1H), 4.23 (d, *J* = 5.2 Hz, 2H), 3.85 – 3.65 (m, 1H), 2.81 – 2.52 (m, 5H),
12 2.47 (s, 3H), 2.33 (s, 3H), 2.07 (s, 6H), 1.93 – 1.79 (m, 1H), 1.70 – 1.55 (m, 1H). MS (ESI) *m/z*
13 593.3 [M+H]⁺ and 591.3 [M-H]⁻.
14
15
16
17
18
19
20
21
22
23
24
25
26

27 ***N*-{3-[(2-Acetyl-1*H*-pyrrolo[2,3-*b*]pyridin-5-ylamino)-methyl]-4-methyl-phenyl}-3-(4-**
28 **methyl-imidazol-1-yl)-5-trifluoromethyl-benzamide (**7z**)**
29
30
31

32 The reaction was carried out as described in general procedure A using **4b** (100 mg, 0.34 mmol),
33 3-(4-methyl-imidazol-1-yl)-5-trifluoromethyl-benzoic acid **5z** (91.8 mg, 0.34 mmol), HATU
34 (258 mg, 0.679 mmol), DIEA (442 μ L, 2.54 mmol) and anhydrous DMF (3 mL). Purification by
35 reverse phase flash chromatography (H₂O/ACN with 1% TFA, 100/0 to 50/50) yielded after
36 neutralization with NaHCO_{3(aq)} and filtration **7z** (13 mg, 7%). ¹H-NMR (400 MHz, DMSO-*d*₆) δ
37 11.80 (s, 1H), 10.49 (s, 1H), 8.43 (s, 1H), 8.38 (s, 1H), 8.18 (s, 1H), 8.14 – 8.10 (m, 2H), 7.75 –
38 7.63 (m, 3H), 7.22 (d, *J* = 8.3 Hz, 1H), 7.06 (d, *J* = 2.1 Hz, 1H), 6.99 (d, *J* = 2.6 Hz, 1H), 6.10 (t,
39 *J* = 5.3 Hz, 1H), 4.25 (d, *J* = 5.3 Hz, 2H), 2.47 (s, 3H), 2.35 (s, 3H), 2.17 (s, 3H). MS (ESI) *m/z*
40 547.2 [M+H]⁺ and 545.1 [M-H]⁻.
41
42
43
44
45
46
47
48
49
50
51
52

53 **5-{2-Methyl-5-[4-(4-methyl-piperazin-1-ylmethyl)-benzoylamino]-benzylamino}-1*H*-**
54 **pyrrolo[2,3-*b*]pyridine-2-carboxylic acid (**8x**)**
55
56
57
58
59
60

Potassium hydroxide (96 mg, 1.71 mmol) was added to a solution of compound **6x** (300 mg, 0.57 mmol) in a mixture of 3 mL methanol and 3 mL water. The mixture was stirred at reflux until the reaction was complete. The solvents were removed, water was added and the mixture was acidified by HCl 6N until pH 7. The precipitate formed was filtered and rinsed with water to give **8x** (222 mg, 76%). ¹H-NMR (300 MHz, DMSO-*d*₆) δ 11.77 (s, 1H), 10.10 (s, 1H), 8.05 (d, *J* = 2.4 Hz, 1H), 7.86 (d, *J* = 8.2 Hz, 2H), 7.69 (s, 1H), 7.65 (dd, *J* = 7.9, 1.6 Hz, 1H), 7.39 (d, *J* = 8.1 Hz, 2H), 7.16 (d, *J* = 8.2 Hz, 1H), 6.98 (d, *J* = 2.4 Hz, 1H), 6.80 (d, *J* = 1.7 Hz, 1H), 5.97 (s, 1H), 4.21 (s, 2H), 3.51 (s, 3H), 2.46 – 2.28 (m, 10H), 2.19 (s, 3H). MS (ESI) *m/z* 513.3 [M+H]⁺ and 511.3 [M-H]⁻.

5-{5-[4-(3-Dimethylamino-pyrrolidin-1-ylmethyl)-3-trifluoromethyl-benzoylamino]-2-methyl-benzylamino}-1*H*-pyrrolo[2,3-*b*]pyridine-2-carboxylic acid (8y**)**

Potassium hydroxide (162 mg, 2.46 mmol) was added to a solution of compound **6y** (500 mg, 0.82 mmol) in a mixture of 3 mL methanol and 3 mL water. The mixture was stirred at reflux until the reaction was complete. The solvents were removed, water was added and the mixture was acidified by HCl 6N until pH 7. The precipitate formed was filtered and rinsed with water to give **8y** (204 mg, 42%). ¹H-NMR (300 MHz, DMSO-*d*₆) δ 11.70 (s, 1H), 10.37 (s, 1H), 8.22 – 8.12 (m, 2H), 8.03 (s, 1H), 7.85 (d, *J* = 8.0 Hz, 1H), 7.66 (bs, 2H), 7.19 (d, *J* = 8.4 Hz, 1H), 6.96 (s, 1H), 6.75 (s, 1H), 6.01 (s, 1H), 4.22 (s, 2H), 3.80 (d, *J* = 14.5 Hz, 1H), 3.72 (d, *J* = 14.5 Hz, 1H), 2.98 – 2.79 (m, 1H), 2.71 – 2.52 (m, 3H), 2.47 – 2.40 (m, 1H), 2.33 (s, 3H), 2.16 (s, 6H), 1.97 – 1.82 (m, 1H), 1.76 – 1.61 (m, 1H). MS (ESI) *m/z* 595.3 [M+H]⁺ and 593.3 [M-H]⁻.

5-{2-Methyl-5-[3-(4-methyl-imidazol-1-yl)-5-trifluoromethyl-benzoylamino]-benzylamino}-1*H*-pyrrolo[2,3-*b*]pyridine-2-carboxylic acid (8z**)**

1
2
3 Lithium hydroxide (38 mg, 1.59 mmol) was added to a solution of compound **6z** (300 mg, 0.53
4 mmol) in a mixture of 4 mL methanol and 4 mL water. The mixture was stirred at reflux until the
5 reaction was complete. The solvents were removed, water was added and the mixture was
6 acidified by HCl 6N until pH 7. The precipitate formed was filtered and rinsed with water to give
7 **8z** (185 mg, 64%). ¹H-NMR (400 MHz, DMSO-*d*₆) δ 11.85 (s, 1H), 10.52 (s, 1H), 9.54 (s, 1H),
8 8.55 (s, 1H), 8.37 (s, 2H), 8.12 (s, 1H), 8.07 (d, *J* = 2.3 Hz, 1H), 7.69 (s, 1H), 7.66 (d, *J* = 8.2 Hz,
9 1H), 7.23 (d, *J* = 8.2 Hz, 1H), 6.98 (s, 1H), 6.83 (d, *J* = 2.3 Hz, 1H), 6.11 (bs, 1H), 4.26 (s, 2H),
10 2.35 (s, 3H), 2.33 (s, 3H). MS (ESI) *m/z* 549.2 [M+H]⁺.
11
12
13
14
15
16
17
18
19
20
21

22 **5-Nitro-1*H*-pyrrolo[2,3-*b*]pyridine-2-carboxylic acid methanamide (10)**

23
24 Potassium hydroxide (895 mg, 13.6 mmol) was added to a solution of 5-nitro-1*H*-pyrrolo[2,3-
25 *b*]pyridine-2-carboxylic acid methyl ester **9** (1.00 g, 4.5 mmol) in a mixture of 15 mL methanol
26 and 15 mL water. The mixture was stirred at reflux until the reaction was complete. The solvents
27 were removed, water was added and the mixture was acidified by HCl 6N until pH 3. The
28 precipitate formed was filtered, rinsed by water and dried under vacuum. The solid (745 mg) was
29 directly used in the next step. Under Argon, the crude was dissolved with 8 mL of dry DMF and
30 HATU (1.62 g, 4.3 mmol) was added followed by DIEA (3.1 mL, 17.8 mmol) and methylamine
31 hydrochloride (715 mg, 10.7 mmol). The reaction mixture was stirred at room temperature
32 overnight. The mixture was concentrated and saturated aqueous solution (50 mL) of Na₂CO₃ was
33 added. The precipitate formed was filtered, rinsed with water and Et₂O and dried under vacuum
34 to obtain **10** (587 mg, 59% over two steps). ¹H-NMR (300 MHz, DMSO-*d*₆) δ 12.96 (s, 1H),
35 9.17 (d, *J* = 2.3 Hz, 1H), 9.06 (d, *J* = 2.3 Hz, 1H), 8.75 (d, *J* = 4.3 Hz, 1H), 7.32 (s, 1H), 2.83 (d,
36 *J* = 4.3 Hz, 3H). MS (ESI) *m/z* 221.1 [M+H]⁺ and 219.1 [M-H]⁻.
37
38
39
40
41
42
43
44
45
46
47
48
49
50
51
52
53
54
55
56
57
58
59
60

1
2
3 **5-(5-Amino-2-methyl-benzylamino)-1H-pyrrolo[2,3-b]pyridine-2-carboxylic acid**
4
5 **methylamide (11)**
6
7

8 In an autoclave under argon, Palladium 10% on charcoal (220 mg, 14% w/w) was added to a
9 solution of 5-nitro-1H-pyrrolo[2,3-b]pyridine-2-carboxylic acid methylamide **10** (1.56 g, 7.1
10 mmol) in 800 mL MeOH. The reaction mixture was stirred overnight at room temperature under
11 hydrogen pressure (30 bars). Then it was filtered through celite, rinsed with MeOH and
12 concentrated. The crude product obtained (880 mg, 65% yield) was directly dissolved in 60 mL
13 MeOH and 6 mL AcOH and 2-methyl-5-nitro-benzaldehyde (764 mg, 4.6 mmol) was added.
14 After 2 h stirring at room temperature, NaBH₃CN (574 mg, 9.3 mmol) was added and the
15 reaction mixture was stirred overnight at room temperature. The mixture was concentrated and
16 slowly neutralized by a saturated aqueous solution of NaHCO₃. The precipitate formed was
17 filtered, rinsed with water and diethyl ether, and dried under vacuum to give the nitro
18 intermediate (1.33g, 84% yield). 500 mg (1.5 mmol) of this crude product was introduced in an
19 autoclave under argon and solubilized with 400 mL of MeOH. Palladium 10% on charcoal (70
20 mg, 14% w/w) was added and the reaction mixture was stirred overnight at room temperature
21 under 30 bars hydrogen pressure. Then it was filtered through celite, rinsed with MeOH and
22 concentrated to obtain **11** (442 mg, 97% yield for the last step, 53% global yield from **10**). ¹H-
23 NMR (300 MHz, DMSO-*d*₆) δ 11.55 (s, 1H), 8.31 (d, *J* = 4.2 Hz, 1H), 7.95 (d, *J* = 2.3 Hz, 1H),
24 6.95 (d, *J* = 2.3 Hz, 1H), 6.82 (d, *J* = 8.0 Hz, 1H), 6.77 (s, 1H), 6.58 (d, *J* = 1.9 Hz, 1H), 6.36
25 (dd, *J* = 8.0, 1.9 Hz, 1H), 5.77 (t, *J* = 5.0 Hz, 1H), 4.76 (s, 2H), 4.07 (d, *J* = 5.0 Hz, 2H), 2.78 (d,
26 *J* = 4.2 Hz, 3H), 2.16 (s, 3H). MS (ESI) *m/z* 310.2 [M+H]⁺.
27
28
29
30
31
32
33
34
35
36
37
38
39
40
41
42
43
44
45
46
47
48
49
50
51
52

53 **5-{2-Methyl-5-[4-(4-methyl-piperazin-1-ylmethyl)-benzoylamino]-benzylamino}-1H-**
54 **pyrrolo[2,3-b]pyridine-2-carboxylic acid methylamide (12x)**
55
56
57
58
59
60

1
2
3 Under argon, 5-(5-amino-2-methyl-benzylamino)-1*H*-pyrrolo[2,3-*b*]pyridine-2-carboxylic acid
4 methylamide **11** (70 mg, 0.23 mmol) was dissolved in 7 mL dry DMF. 4-[(4-methyl-1-
5 piperazinyl)methyl]benzoic acid **5x** (70 mg, 0.30 mmol) was added followed by HATU (95 mg,
6 0.25 mmol) and DIEA (231 μ L, 1.33 mmol). The reaction mixture was stirred at room
7 temperature overnight. Then the mixture was concentrated and neutralized by a saturated
8 aqueous solution of NaHCO₃. The precipitate formed was filtered and purified on a reverse
9 chromatography column (H₂O/ACN with 1% TFA, 100/0 to 0/100) to give after neutralization
10 with NaHCO_{3(aq)} and filtration **12x** (4 mg, 3%). ¹H-NMR (400 MHz, DMSO-*d*₆) δ 11.51 (s, 1H),
11 10.09 (s, 1H), 8.26 (d, *J* = 4.4 Hz, 1H), 7.98 (s, 1H), 7.85 (d, *J* = 8.1 Hz, 2H), 7.70 (s, 1H), 7.64
12 (d, *J* = 7.8 Hz, 1H), 7.39 (d, *J* = 8.1 Hz, 2H), 7.16 (d, *J* = 7.8 Hz, 1H), 6.99 (d, *J* = 2.0 Hz, 1H),
13 6.77 (d, *J* = 2.0 Hz, 1H), 5.87 (t, *J* = 5.2 Hz, 1H), 4.21 (d, *J* = 5.2 Hz, 2H), 3.50 (s, 3H), 2.78 (d,
14 *J* = 4.4 Hz, 3H), 2.32 (bs, 10H), 2.15 (s, 3H). MS (ESI) *m/z* 526.3 [M+H]⁺. HPLC purity: 94%.

15
16
17
18
19
20
21
22
23
24
25
26
27
28
29
30
31
32 **5-{5-[4-(3-Dimethylamino-pyrrolidin-1-ylmethyl)-3-trifluoromethyl-benzoylamino]-2-**
33 **methyl-benzylamino}-1*H*-pyrrolo[2,3-*b*]pyridine-2-carboxylic acid methylamide (**12y**)**

34 Under argon, 5-(5-amino-2-methyl-benzylamino)-1*H*-pyrrolo[2,3-*b*]pyridine-2-carboxylic acid
35 methylamide **11** (70 mg, 0.23 mmol) was dissolved in 7 mL dry DMF. 4-(3-dimethylamino-
36 pyrrolidin-1-ylmethyl)-3-trifluoromethyl-benzoic acid **5y** (70 mg, 0.22 mmol) was added
37 followed by HATU (94 mg, 0.25 mmol), DIEA (231 μ L, 1.33 mmol). The reaction mixture was
38 stirred at room temperature overnight. Then it was concentrated and neutralized by a saturated
39 aqueous solution of NaHCO₃. The precipitate formed was filtered and purified on a reverse
40 chromatography column (H₂O/ACN with 1% TFA, 100/0 to 0/100) to give after neutralization
41 with NaHCO_{3(aq)} and filtration **12y** (9 mg, 7%). ¹H-NMR (400 MHz, DMSO-*d*₆) δ 11.51 (s, 1H),
42 10.33 (s, 1H), 8.29 – 8.23 (m, 1H), 8.18 (s, 1H), 8.17 (d, *J* = 8.3 Hz, 1H), 7.98 (d, *J* = 2.5 Hz,
43 44 45 46 47 48 49 50 51 52 53 54 55 56 57 58 59 60

1
2
3 1H), 7.85 (d, $J = 7.9$ Hz, 1H), 7.68 (d, $J = 1.8$ Hz, 1H), 7.65 (dd, $J = 7.9, 2.0$ Hz, 1H), 7.19 (d, J
4 = 8.3 Hz, 1H), 6.99 (d, $J = 2.5$ Hz, 1H), 6.77 (d, $J = 2.0$ Hz, 1H), 5.90 (t, $J = 5.5$ Hz, 1H), 4.23
5
6 (d, $J = 5.5$ Hz, 2H), 3.78 (d, $J = 15.1$ Hz, 1H), 3.74 (d, $J = 15.1$ Hz, 1H), 2.78 (d, $J = 4.6$ Hz, 3H),
7
8 2.76 – 2.53 (m, 4H), 2.40 – 2.30 (m, 1H), 2.40 – 2.30 (m, 3H), 2.12 – 2.05 (m, 6H), 1.92 – 1.82
9
10 (m, 1H), 1.68 – 1.58 (m, 1H). MS (ESI) m/z 608.2 $[M+H]^+$.

15 **5-formyl-1H-pyrrolo[2,3-*b*]pyridine-2-carboxylic acid methyl ester (14a)**

16
17 5-Cyano-1H-pyrrolo[2,3-*b*]pyridine-2-carboxylic acid methyl ester **13a** (200 mg, 1 mmol) in
18 solution in a mixture of pyridine/H₂O/AcOH (2/1/1, 150 mL) was stirred with 0.5 mL of Raney
19 Nickel in water under a 10 bar pressure of hydrogen. The mixture was filtered over celite and
20 washed with MeOH. The filtrate was concentrated, washed with a saturated aqueous solution of
21 NaHCO₃ and extracted with AcOEt to give **14a** as a brown solid (137mg, 67%). ¹H-NMR (300
22 MHz, DMSO-*d*₆) δ 13.06 (bs, 1H), 10.11 (s, 1H), 8.92 (d, $J = 1.7$ Hz, 1H), 8.66 (d, $J = 1.7$ Hz,
23 1H), 7.39 (s, 1H), 3.90 (s, 3H). MS (ESI) m/z 205.1 $[M+H]^+$.

34 **2-acetyl-1H-pyrrolo[2,3-*b*]pyridine-5-carbaldehyde (14b)**

35
36 2-Acetyl-1H-pyrrolo[2,3-*b*]pyridine-5-carbonitrile **10b** (4.02 g, 22 mmol) in dry toluene was
37 cooled down at 0°C, and DIBAL-H 1M in cyclohexane (65 mL, 65 mmol) was added dropwise.
38 The mixture was stirred at 0°C for 1h30. Then, 85 mL of MeOH were cautiously added,
39 followed by 25.5 mL of a 2M solution of H₂SO₄. The aluminum salts were filtered on celite. The
40 filtrate was concentrated and the residue purified by column chromatography on silica gel
41 (Petroleum ether/AcOEt from 6/4 to 0/10) to give 2-(1-Hydroxy-ethyl)-1H-pyrrolo[2,3-
42 *b*]pyridine-5-carbaldehyde as a yellow solid (1.3 g, 6.8 mmol, 31% yield). This solid was
43 directly dissolved in THF (130 mL). Activated MnO₂ (7.1 g, 82 mmol) was cautiously added and
44 the mixture was stirred overnight at room temperature. The MnO₂ was eliminated by filtration on
45
46
47
48
49
50
51
52
53
54
55
56
57
58
59
60

1
2
3 celite, rinsed by hot methanol and DMF (200 mL). The filtrate was concentrated and the
4
5 resulting off-white solid was washed with diethyl ether to give **14b** (844 mg, 65%). ¹H-NMR
6
7 (300 MHz, DMSO-*d*₆) δ 12.83 (s, 1H), 10.11 (s, 1H), 8.93 (d, *J* = 1.9 Hz, 1H), 8.70 (d, *J* = 1.9
8
9 Hz, 1H), 7.58 (s, 1H), 2.60 (s, 3H). MS (ESI) *m/z* 189.1 [M+H]⁺ and 187.1 [M-H]⁻.

5-hydroxymethyl-1*H*-pyrrolo[2,3-*b*]pyridine-2-carboxylic acid methyl ester (**15a**)

14
15 Under argon, a solution of 5-formyl-1*H*-pyrrolo[2,3-*b*]pyridine-2-carboxylic acid methyl ester
16
17 **14a** (667 mg, 3.3 mmol) in dry THF (35 mL) was cooled down at 0°C and a solution of DIBAL-
18
19 H in cyclohexane 1M (9.8 mL, 9.8 mmol) in dry THF (17 mL) was slowly added. The mixture
20
21 was stirred at 0°C for 3 h then quenched by addition of water. The mixture was concentrated and
22
23 the crude was washed with NaHCO_{3(aq)} and extracted by AcOEt. Organic layer was dried with
24
25 Na₂SO₄ and AcOEt was evaporated under reduced pressure. The crude was purified by column
26
27 chromatography on silica gel (petroleum ether/AcOEt/MeOH, 100/0/0 to 0/100/0 to 0/97/3) to
28
29 give **15a** (304 mg, 45%) ¹H NMR (300 MHz, DMSO-*d*₆) δ 12.45 (s, 1H), 8.38 (d, *J* = 2.0 Hz,
30
31 1H), 8.02 (d, *J* = 2.0 Hz, 1H), 7.16 (s, 1H), 5.24 (t, *J* = 5.6 Hz, 1H), 4.59 (d, *J* = 5.6 Hz, 2H),
32
33 3.87 (s, 3H). MS (ESI) *m/z* 207.1 [M+H]⁺.

5-(5-amino-2-methyl-phenoxy-methyl)-1*H*-pyrrolo[2,3-*b*]pyridine-2-carboxylic acid methyl ester (**16a**)

34
35 To a solution of 2-methyl-5-nitrophenol (147 mg, 0.96 mmol) in dry CH₂Cl₂ (4 mL) under
36
37 argon was added PPh₃ (252 mg, 0.96 mmol) followed by 5-hydroxymethyl-1*H*-pyrrolo[2,3-
38
39 *b*]pyridine-2-carboxylic acid methyl ester **12** (180 mg, 0.87 mmol). A solution of DEAD (104
40
41 μL, 0.66 mmol) in CH₂Cl₂ (2 mL) was slowly added and the mixture was stirred at room
42
43 temperature overnight. The crude was filtered and the precipitate was washed with CH₂Cl₂. The
44
45 crude product (120 mg, yield: 40%) was used directly in the next step without purification step.
46
47
48
49
50
51
52
53
54
55
56
57
58
59
60

1
2
3 After dissolution in a AcOH/AcOEt mixture (1/2, 5 mL), zinc powder (317 mg, 4.8 mmol) was
4 added. The mixture was stirred at 50°C for 1h30. The reaction mixture was filtered on celite and
5 washed with NaHCO₃ aqueous solution. After drying, the intermediate **16a** (137 mg, yield >
6 100%) was directly used without supplementary purification in the next step. ¹H-NMR (300
7 MHz, DMSO-*d*₆) δ 8.50 (d, *J* = 1.7 Hz, 1H), 8.17 (d, *J* = 1.7 Hz, 1H), 7.20 (s, 1H), 6.76 (d, *J* =
8 7.9 Hz, 1H), 6.34 (d, *J* = 0.9 Hz, 1H), 6.07 (dd, *J* = 7.9, 1.8 Hz, 1H), 5.09 (s, 2H), 4.85 (s, 2H),
9 3.88 (s, 3H), 1.99 (s, 3H). MS (ESI) *m/z* 312.2 [M+H]⁺. HPLC purity: 81%.

19
20 **5-[2-(2-Methyl-5-nitro-phenyl)-vinyl]-1*H*-pyrrolo[2,3-*b*]pyridine-2-carboxylic acid**
21
22 **methyl ester (17a)**

23
24 A solution of 5-Formyl-1*H*-pyrrolo[2,3-*b*]pyridine-2-carboxylic acid methyl ester **14a** (1.0 g,
25 4.9 mmol), (2-methyl-5-nitro-benzyl)-triphenyl-phosphonium (2.7 g, 5.5 mmol) and LiOH (294
26 mg, 12.3 mmol) in anhydrous MeOH (100mL) was stirred at reflux overnight. The precipitate
27 was filtered and washed with MeOH before purification on reverse phase flash chromatography
28 (H₂O/ACN) to give **17a** (769 mg, 69%) as a mixture of two isomers. ¹H-NMR (300 MHz,
29 DMSO-*d*₆), stereoisomer ratio ~ 7/3, δ 12.76 – 12.15 (m, 1H), 8.79 (s, 0.3H), 8.49 (s, 0.7H),
30 8.15 – 8.00 (m, 2H), 7.92 – 7.75 (m, 1H), 7.60 – 7.47 (m, 1H), 7.20 (s, 0.3H), 7.07 (s, 0.7H),
31 6.96 (d, *J* = 12.1 Hz, 1H), 6.77 (d, *J* = 12.1 Hz, 1H), 3.89 (s, 0.9H), 3.85 (s, 2.1H), 2.56 (s, 0.9H),
32 2.36 (s, 2.1H). MS (ESI) *m/z* 338.1 [M+H]⁺ and 336.1 [M-H]⁻. HPLC stereoisomer ratio: 8/2.

33
34
35
36
37
38
39
40
41
42
43
44
45
46 **1-[5-[2-(2-Methyl-5-nitro-phenyl)-vinyl]-1*H*-pyrrolo[2,3-*b*]pyridin-2-yl]-ethanone (17b)**

47
48 A solution of 2-acetyl-1*H*-pyrrolo[2,3-*b*]pyridine-5-carbaldehyde **14b** (844 mg, 4.5 mmol), (2-
49 Methyl-5-nitro-benzyl)-triphenyl-phosphonium (2.4 g, 4.9 mmol) and LiOH (215 mg, 9.0 mmol)
50 in anhydrous MeOH (150 mL) was stirred at room temperature overnight. The precipitate was
51 filtered, washed with NH₄Cl aqueous solution, water and Et₂O to obtain **17b** as a yellow solid
52
53
54
55
56
57
58
59
60

1
2
3 (1.03 g, 71%) that was directly used in the next step without further purification. ¹H-NMR (300
4 MHz, DMSO-*d*₆) δ 12.31 (s, 1H), 8.14 (d, *J* = 1.4 Hz, 1H), 8.05 (dd, *J* = 8.4, 1.8 Hz, 1H), 7.85
5 (d, *J* = 1.8 Hz, 1H), 7.80 (d, *J* = 1.4 Hz, 1H), 7.55 (d, *J* = 8.4 Hz, 1H), 7.24 (s, 1H), 6.96 (d, *J* =
6 12.1 Hz, 1H), 6.76 (d, *J* = 12.1 Hz, 1H), 2.50 (s, 3H), 2.34 (s, 3H). MS (ESI) *m/z* 322.1 [M+H]⁺
7 and 320.1 [M-H]⁻. HPLC purity: 88%.
8
9

10
11
12
13
14
15 **5-[2-(5-amino-2-methyl-phenyl)-ethyl]-1*H*-pyrrolo[2,3-*b*]pyridine-2-carboxylic acid methyl**
16 **ester (18a)**
17

18
19
20 5-[2-(2-Methyl-5-nitro-phenyl)-vinyl]-1*H*-pyrrolo[2,3-*b*]pyridine-2-carboxylic acid methyl
21 ester **17a** (283 mg, 0.84 mmol) was dissolved in AcOH/AcOEt mixture (1/2, 6 mL). Zinc (819
22 mg, 12.6 mmol) was added and the mixture was put in sonic bath at room temperature for 30
23 minutes. Then, the mixture was filtered over celite and washed with AcOEt. The filtrate was
24 concentrated and purified on reverse phase flash chromatography (H₂O/ACN with 1% TFA,
25 100/0 to 0/100) to give after neutralization with NaHCO_{3(aq)} and filtration **18a** (144 mg, 56%) as
26 a mixture of two stereoisomers. ¹H-NMR (300 MHz, DMSO-*d*₆), stereoisomer ratio ~ 8/2, δ
27 12.55 (s, 0.2H), 12.47 (s, 0.8H), 8.67 (s, 0.2H), 8.35 (s, 0.2H), 8.16 (s, 0.8H), 7.82 (s, 0.8H), 7.38
28 (d, *J* = 16.6 Hz, 0.2H), 7.17 (s, 0.2H), 7.10 – 7.00 (m, 1.0 H), 6.95 – 6.83 (m, 1.2 H), 6.73 – 6.56
29 (m, 1.6 H), 6.50 – 6.37 (m, 1.0H), 6.37 – 6.28 (s, 0.8H) 4.80 (bs, 2H), 3.89 (s, 0.6H), 3.85 (s,
30 2.4H), 2.26 (s, 0.6H), 2.04 (s, 2.4H). MS (ESI) *m/z* 189.1 [M+H]⁺ and 187.1 [M-H]⁻.
31
32
33
34
35
36
37
38
39
40
41
42
43
44
45

46 **5-[2-(5-Amino-2-methyl-phenyl)-ethyl]-1*H*-pyrrolo[2,3-*b*]pyridine-2-carboxylic acid**
47 **methyl ester (19a)**
48

49
50 5-[2-(2-Methyl-5-nitro-phenyl)-vinyl]-1*H*-pyrrolo[2,3-*b*]pyridine-2-carboxylic acid methyl
51 ester **17a** (450 mg, 1.3 mmol) was dissolved in DMF (180 mL) with Pd/C 10% (90 mg, 20%
52 w/w) and stirred for 24 h under hydrogen pressure (10 bars). The reaction mixture was then
53
54
55
56
57
58
59
60

1
2
3 filtered over celite bed. The crude product was purified on reverse phase column
4 chromatography (H₂O/ACN with 1% TFA, 100/0 to 0/100) to give after neutralization with
5 NaHCO_{3(aq)} and filtration **19a** (157mg, 26%). ¹H-NMR (300 MHz, DMSO-*d*₆) δ 12.39 (s, 1H),
6 8.28 (s, 1H), 7.93 (s, 1H), 7.11 (s, 1H), 6.77 (d, *J* = 8.0 Hz, 1H), 6.43 (d, *J* = 2.1 Hz, 1H), 6.32
7 (dd, *J* = 8.0, 2.1 Hz, 1H), 4.73 (s, 2H), 3.87 (s, 3H), 2.93 – 2.80 (m, 2H), 2.79 – 2.68 (m, 2H),
8 2.08 (s, 3H). MS (ESI) *m/z* 310.2 [M+H]⁺ and 308.1 [M-H]⁻.

9
10
11
12
13
14
15
16
17
18 **1-{5-[2-(5-Amino-2-methyl-phenyl)-ethyl]-1*H*-pyrrolo[2,3-*b*]pyridin-2-yl}-ethanone (19b)**

19
20 1-{5-[2-(2-Methyl-5-nitro-phenyl)-vinyl]-1*H*-pyrrolo[2,3-*b*]pyridin-2-yl}-ethanone **17b** (845
21 mg, 2.6 mmol) was dissolved in DMF (400 mL) with 10% Pd/C (90 mg, 10% w/w) and stirred
22 overnight under hydrogen pressure (10 bars). The reaction mixture was then filtered on celite and
23 concentrated to afford a brown powder which was further purified on column chromatography
24 (H₂O/ACN with 1% TFA, 100/0 to 0/100) to give after neutralization with NaHCO_{3(aq)} and
25 filtration **19b** (364 mg, 38%). ¹H-NMR (300 MHz, DMSO- *d*₆) δ 12.16 (s, 1H), 8.29 (s, 1H),
26 7.94 (s, 1H), 7.28 (s, 1H), 6.77 (d, *J* = 8.0 Hz, 1H), 6.43 (s, 1H), 6.32 (d, *J* = 8.0 Hz, 1H), 4.72 (s,
27 2H), 2.92 – 2.83 (m, 2H), 2.78 – 2.68 (m, 2H), 2.55 (s, 3H), 2.07 (s, 3H). MS (ESI) *m/z* 294.2
28 [M+H]⁺.

29
30
31
32
33
34
35
36
37
38
39
40
41 **5-(2-methyl-5-nitrobenzamido)-1*H*-pyrrolo[2,3-*b*]pyridine-2-carboxylic acid methyl ester**
42
43
44 **(21a)**

45
46 5-Amino-1*H*-pyrrolo[2,3-*b*]pyridine-2-carboxylic acid methyl ester **1a** (5.74 g, 30 mmol) and
47 2-methyl-5-nitrobenzoic acid **20** (5.44 g, 30 mmol) were stirred in DMF (300 mL) at room
48 temperature. HATU (11.42 g, 30 mmol) and DIEA (26 mL, 150 mmol) were added and the
49 mixture was stirred for the week-end at room temperature. The solvent was evaporated and
50 saturated NaHCO₃ aqueous solution was added until obtaining a precipitate that was filtered and
51
52
53
54
55
56
57
58
59
60

1
2
3 washed with water followed by a mixture of petroleum ether/diethyl ether (1/1). After drying
4 under vacuum, the nitro intermediate was obtained as powder (9.94 g, yield: 93%) and directly
5 used in the reduction step. The powder was dissolved in methanol with Pd/C 10% (0.95 g, 10%
6 w/w) and the mixture was stirred under hydrogen pressure (35 bars) at room temperature
7 overnight. Then, the mixture was filtered over celite bed that was washed with hot methanol (~ 2
8 L). The filtrate was concentrated to give the expected product **21a** (7.35 g, 81%). ¹H-NMR (300
9 MHz, DMSO-*d*₆) δ 10.29 (s, 1H), 8.57 – 8.52 (m, 2H), 7.15 (s, 1H), 6.94 (d, *J* = 8.2 Hz, 1H),
10 6.71 (d, *J* = 2.3 Hz, 1H), 6.59 (dd, *J* = 8.2, 2.3 Hz, 1H), 5.08 (s, 2H), 3.86 (s, 3H), 2.21 (s, 3H).
11
12 MS (ESI) *m/z* 325.2 [M+H]⁺.
13
14
15
16
17
18
19
20
21
22
23

24 ***N*-(3-Amino-4-methyl-phenyl)-4-(4-methyl-piperazin-1-ylmethyl)-benzamide (23x)**

25
26 A solution of 4-methyl-3-nitroaniline **22** (250 mg, 1.6 mmol), 4-(4-methyl-piperazin-1-
27 ylmethyl)-benzoic acid **5x** (769 mg, 3.2mmol) and DIEA (860 μL, 4.8 mmol) in dry DMF was
28 stirred at room temperature for 15 minutes. EDCI (471 mg, 2.4 mmol) was added and the
29 mixture was stirred overnight at room temperature. Then, the solvent was evaporated and the
30 crude mixture was washed with saturated NaHCO₃ aqueous solution and extracted with AcOEt.
31 The organic layer was dried over Na₂SO₄, filtered and concentrated. The crude product was
32 purified on flash column chromatography on silica gel (CH₂Cl₂/MeOH, 100/0 to 75/25) to give a
33 yellow solid (270 mg, yield: 45%). 230 mg of this powder were directly dissolved in a mixture
34 AcOEt/AcOH (2/1). Activated Zn (613 mg) was added and the mixture was stirred at room
35 temperature for 1h20. The, Zn residue was filtered over celite and the filtrate was concentrated.
36 The crude mixture was dissolved in water, then basified by addition of NaHCO₃ until pH 7-8 and
37 extracted with AcOEt. The organic layer was dried over Na₂SO₄, filtered and concentrated to
38 give **23x** (238 mg, reduction yield: quantitative). ¹H-NMR (300 MHz, DMSO-*d*₆) δ 9.86 (s, 1H),
39
40
41
42
43
44
45
46
47
48
49
50
51
52
53
54
55
56
57
58
59
60

1
2
3 7.86 (d, $J = 8.0$ Hz, 2H), 7.40 (d, $J = 8.0$ Hz, 2H), 7.11 (d, $J = 1.4$ Hz, 1H), 6.91 – 6.73 (m, 2H),
4
5 4.83 (s, 2H), 3.52 (s, 2H), 2.47 – 2.25 (m, 8H), 2.19 (s, 3H), 2.01 (s, 3H). MS (ESI) m/z 339.3
6
7
8 $[M+H]^+$ and 337.3 $[M-H]^-$.
9

10 **5-({2-Methyl-5-[4-(4-methyl-piperazin-1-ylmethyl)-benzoylamino]-phenylamino}-**
11
12 **methyl)-1*H*-pyrrolo[2,3-*b*]pyridine-2-carboxylic acid methyl ester (25x)**
13
14

15 Under argon, 5-formyl-1*H*-pyrrolo[2,3-*b*]pyridine-2-carboxylic acid methyl ester **14a** (106
16 mg, 0.33 mmol) and *N*-(3-Amino-4-methyl-phenyl)-4-(4-methyl-piperazin-1-ylmethyl)-
17 benzamide **23x** (113 mg, 0.33 mmol) were dissolved in a mixture of MeOH (2 mL) and AcOH
18 (200 μ l). The mixture was stirred at room temperature for 2 h. Then, NaBH₃CN (41 mg, 0.66
19 mmol) was added and the mixture was stirred overnight at room temperature. The precipitate
20 was filtered and washed with MeOH and Et₂O to give **25x** (30 mg, 17%). ¹H-NMR (400 MHz,
21 DMSO-*d*₆) δ 12.44 (s, 1H), 9.85 (s, 1H), 8.48 (d, $J = 2.0$ Hz, 1H), 8.05 (d, $J = 1.6$ Hz, 1H), 7.83
22 (d, $J = 8.2$ Hz, 2H), 7.40 (d, $J = 8.2$ Hz, 2H), 7.14 (d, $J = 2.0$ Hz, 1H), 7.02 – 6.96 (m, 2H), 6.91
23 (d, $J = 7.8$ Hz, 1H), 5.67 (t, $J = 5.9$ Hz, 1H), 4.44 (d, $J = 5.9$ Hz, 2H), 3.85 (s, 3H), 3.57 (s, 2H),
24 3.10-2.55 (m, 8H), 2.13 (s, 3H), 2.08 (s, 2H). MS (ESI) m/z 527 $[M+H]^+$.
25
26
27
28
29
30
31
32
33
34
35
36
37

38 **General procedure C for coupling reaction to obtain compounds 24x-y and 26x-y to 29x-y**
39

40 All the reactants (carboxylic acid reactant, aniline intermediate, HATU and DIEA) were placed
41 in dried schlenck under argon and stirred in DMF at room temperature overnight. DMF was
42 evaporated and saturated NaHCO₃ aqueous solution was added. The resulting precipitate was
43 filtered and purified by washing with MeOH or by flash column chromatography to obtain the
44 expected product.
45
46
47
48
49
50
51

52 **5-{2-Methyl-5-[4-(4-methyl-piperazin-1-ylmethyl)-benzoylamino]-benzoylamino}-1*H*-**
53
54 **pyrrolo[2,3-*b*]pyridine-2-carboxylic acid methyl ester (24x)**
55
56
57
58
59
60

1
2
3 The reaction was carried out as described in general procedure C using **21a** (2.0 g, 6.2 mmol),
4 4-[(4-methyl-1-piperazinyl)methyl]benzoic acid **5x** (2.8 g, 11.7 mmol), HATU (4.7 g, 12.3
5 mmol), DIEA (5.5 mL, 31 mmol) and anhydrous DMF (100 mL). Purification by reverse phase
6 flash chromatography (H₂O/ACN with 1% TFA, 100/0 to 0/100) yielded after neutralization with
7 NaHCO_{3(aq)} and filtration **24x** (500 mg, 15%). ¹H-NMR (300 MHz, DMSO-*d*₆) δ 12.48 (s, 1H),
8 10.52 (s, 1H), 10.36 (s, 1H), 8.60 (s, 2H), 8.00 – 7.95 (m, 2H), 7.93 (s, 1H), 7.84 (dd, *J* = 2.1, 8.3
9 Hz, 1H), 7.44 (d, *J* = 8.3 Hz, 2H), 7.29 (d, *J* = 8.3 Hz, 1H), 7.20 (s, 1H), 3.88 (s, 3H), 3.53 (s,
10 2H), 2.45 – 2.22 (m, 11H), 2.14 (s, 3H). MS (ESI) *m/z* 541.3 [M+H]⁺ and 539.2 [M-H]⁻.

11
12
13
14
15
16
17
18
19
20
21
22
23
24
25
26
27
28
29
30
31
32
33
34
35
36
37
38
39
40
41
42
43
44
45
46
47
48
49
50
51
52
53
54
55
56
57
58
59
60

5-{5-[4-(3-Dimethylamino-pyrrolidin-1-ylmethyl)-3-trifluoromethyl-benzoylamino]-2-methyl-benzoylamino}-1H-pyrrolo[2,3-*b*]pyridine-2-carboxylic acid methyl ester (24y**)**

The reaction was carried out as described in general procedure C using **21a** (2.0 g, 6.2 mmol),
4-(3-dimethylamino-pyrrolidin-1-ylmethyl)-3-trifluoromethyl-benzoic acid **5y** (2.3 g, 7.4 mmol),
HATU (4.8 g, 12.3 mmol), DIEA (5.5 mL, 31 mmol) and anhydrous DMF (100 mL).
Purification by reverse phase flash chromatography (H₂O/ACN with 1% TFA, 100/0 to 0/100)
yielded after neutralization with NaHCO_{3(aq)} and filtration **24y** (1.1 g, 29%). ¹H-NMR (300 MHz,
DMSO-*d*₆) δ 12.50 (s, 1H), 10.55 (s, 1H), 10.52 (s, 1H), 8.60 (s, 2H), 8.28 – 8.21 (m, 2H), 7.97 –
7.80 (m, 3H), 7.33 (d, *J* = 8.4 Hz, 1H), 7.21 (d, *J* = 1.9 Hz, 1H), 3.88 (s, 3H), 3.85 – 3.70 (m,
2H), 2.92 – 2.77 (m, 1H), 2.76 – 2.54 (m, 4H), 2.39 (s, 3H), 2.14 (s, 6H), 1.95 – 1.83 (m, 1H),
1.75 – 1.60 (m, 1H). MS (ESI) *m/z* 623.2 [M+H]⁺ and 621.2 [M-H]⁻. HPLC purity: 94%.

5-{2-Methyl-5-[4-(4-methyl-piperazin-1-ylmethyl)-benzoylamino]-phenoxy-methyl}-1H-pyrrolo[2,3-*b*]pyridine-2-carboxylic acid methyl ester (26x**)**

The reaction was carried out as described in general procedure C using **16a** (72 mg, 0.25
mmol), 4-[(4-methyl-1-piperazinyl)methyl]benzoic acid **5x** (74 mg, 0.32 mmol), HATU (114

1
2
3 mg, 0.30 mmol), DIEA (216 μ L, 1.24 mmol) and anhydrous DMF (2.5 mL). Purification by
4 reverse phase flash chromatography (H₂O/ACN with 1% TFA, 100/0 to 0/100) yielded after
5 neutralization with NaHCO_{3(aq)} and filtration **26x** (6 mg, 5%). ¹H-NMR (400 MHz, DMSO-*d*₆) δ
6 10.13 (s, 1H), 8.55 (d, *J* = 1.6 Hz, 1H), 8.22 (d, *J* = 1.6 Hz, 1H), 7.90 (d, *J* = 8.2 Hz, 2H), 7.64
7 (d, *J* = 1.5 Hz, 1H), 7.43 (d, *J* = 8.2 Hz, 2H), 7.30 (dd, *J* = 8.1, 1.5 Hz, 1H), 7.20 (s, 1H), 7.10 (d,
8 *J* = 8.1 Hz, 1H), 5.19 (s, 2H), 3.88 (s, 3H), 3.55 – 3.50 (m, 2H), 2.44 – 2.24 (m, 8H), 2.15 (s,
9 3H), 2.13 (s, 3H). MS (ESI) *m/z* 528.3[M+H]⁺ and 526.3 [M-H]⁻.

10
11
12
13
14
15
16
17
18
19
20
21
22 **5-{5-[4-(3-Dimethylamino-pyrrolidin-1-ylmethyl)-3-trifluoromethyl-benzoylamino]-2-**
23 **methyl-phoxymethyl}-1*H*-pyrrolo[2,3-*b*]pyridine-2-carboxylic acid methyl ester (26y)**

24
25 The reaction was carried out as described in general procedure C using **16a** (77 mg, 0.25
26 mmol), 4-(3-dimethylamino-pyrrolidin-1-ylmethyl)-3-trifluoromethyl-benzoic acid **5y** (95 mg,
27 0.30 mmol), HATU (114 mg, 0.30 mmol), DIEA (216 μ L, 1.24 mmol) and anhydrous DMF (2.5
28 mL). Purification by reverse phase flash chromatography (H₂O/ACN with 1% TFA, 100/0 to
29 0/100) yielded after neutralization with NaHCO_{3(aq)} and filtration **26y** (16 mg, 21%). ¹H-NMR
30 (300 MHz, DMSO-*d*₆) δ 10.40 (s, 1H), 8.54 (s, 1H), 8.26 – 8.18 (m, 3H), 7.90 (d, *J* = 7.9 Hz,
31 1H), 7.63 (s, 1H), 7.30 (d, *J* = 7.8 Hz, 1H), 7.19 (s, 1H), 7.13 (d, *J* = 7.8 Hz, 1H), 5.20 (s, 2H),
32 3.87 (s, 3H), 3.88 – 3.70 (m, 2H), 2.81 – 2.57 (m, 4H), 2.43 – 2.33 (m, 1H), 2.14 (s, 3H), 2.09 (s,
33 6H), 1.96 – 1.80 (m, 1H), 1.74 – 1.57 (m, 1H). MS (ESI) *m/z* 305.7 [M+2H]²⁺.

34
35
36
37
38
39
40
41
42
43
44
45
46
47 **5-(-2-{2-Methyl-5-[4-(4-methyl-piperazin-1-ylmethyl)-benzoylamino]-phenyl}-vinyl)-1*H*-**
48 **pyrrolo[2,3-*b*]pyridine-2-carboxylic acid methyl ester (27x)**

49
50 The reaction was carried out as described in general procedure C using **18a** (72 mg, 0.24
51 mmol), 4-[(4-methyl-1-piperazinyl)methyl]benzoic acid **5x** (71 mg, 0.30 mmol), HATU (98 mg,
52 0.26 mmol), DIEA (204 μ L, 1.17 mmol) and anhydrous DMF (3.5 mL). The final compound **27x**
53
54
55
56
57
58
59
60

(57 mg, 46%) was isolated from crude after neutralization with $\text{NaHCO}_3(\text{aq})$, washing with water and filtration as a mixture of isomers. $^1\text{H-NMR}$ (300 MHz, $\text{DMSO-}d_6$), stereoisomer ratio ~25/75, δ 12.59 (s, 0.25H), 12.48 (s, 0.75H), 10.17 (s, 0.25H), 10.04 (s, 0.75H), 8.73 – 8.69 (m, 0.25H), 8.44 – 8.40 (m, 0.25H), 8.17 – 8.14 (m, 0.75H), 8.09 (s, 0.25H), 7.94 (d, $J = 7.8$ Hz, 0.5H), 7.85 (s, 0.75H), 7.80 (d, $J = 8.2$ Hz, 1.5H), 7.72 – 7.66 (m, 0.75H), 7.61 (d, $J = 7.7$ Hz, 0.25H), 7.56 – 7.52 (m, 0.75H), 7.50 – 7.42 (m, 0.5H), 7.37 (d, $J = 8.2$ Hz, 1.5H), 7.28 – 7.10 (m, 1.75H), 7.05 (s, 0.75H), 6.79 (d, $J = 12.3$ Hz, 0.75H), 6.72 (d, $J = 12.3$ Hz, 0.75H), 3.89 (s, 0.75H), 3.84 (s, 2.25H), 3.54 (s, 0.5H), 3.49 (s, 1.5H), 2.44 – 2.22 (m, 8H), 2.21 – 2.10 (m, 6H). MS (ESI) m/z 524.3 $[\text{M}+\text{H}]^+$.

5-(2-{5-[4-(3-Dimethylamino-pyrrolidin-1-ylmethyl)-3-trifluoromethyl-benzoylamino]-2-methyl-phenyl}-vinyl)-1*H*-pyrrolo[2,3-*b*]pyridine-2-carboxylic acid methyl ester (27y)

The reaction was carried out as described in general procedure C using **18a** (55 mg, 0.18 mmol), 4-(3-dimethylamino-pyrrolidin-1-ylmethyl)-3-trifluoromethyl-benzoic acid **5y** (74 mg, 0.23 mmol), HATU (75 mg, 0.20 mmol), DIEA (156 μL , 0.90 mmol) and anhydrous DMF (2.5 mL). Purification by reverse phase flash chromatography ($\text{H}_2\text{O}/\text{ACN}$ with 1% TFA, 100/0 to 0/100) yielded after neutralization with $\text{NaHCO}_3(\text{aq})$ and filtration **26y** (10 mg, 9%) as a mixture of isomers ($Z/E \sim 25/75$). $^1\text{H-NMR}$ (300 MHz, $\text{DMSO-}d_6$) δ 12.59 (s, 0.25H), 12.48 (s, 0.75H), 10.42 (s, 0.25H), 10.27 (s, 0.75H), 8.72 (s, 0.25H), 8.42 (d, $J = 1.8$ Hz, 0.25H), 8.31 – 8.22 (m, 0.5H), 8.17 – 8.03 (m, 2.5H), 7.91 (d, $J = 8.1$ Hz, 0.25H), 7.88 – 7.79 (m, 1.5H), 7.69 (dd, $J = 8.3, 1.8$ Hz, 0.75H), 7.61 (dd, $J = 8.1, 1.8$ Hz, 0.25H), 7.56 – 7.48 (m, 1H), 7.29 – 7.11 (m, 1.5H), 7.05 (s, 0.75H), 6.80 (d, $J = 12.3$ Hz, 0.75H), 6.73 (d, $J = 12.3$ Hz, 0.75H), 3.89 (s, 0.75H), 3.84 (s, 2.25H), 3.79 (d, $J = 15.4$ Hz, 1H), 3.71 (d, $J = 15.4$ Hz, 1H), 2.82 – 2.52 (m,

1
2
3 3H), 2.44 – 2.30 (m, 2H), 2.19 (s, 2.25H), 2.09 (s, 1.5H), 2.07 (s, 4.5H), 1.99 (s, 0.75H), 1.92 –
4
5 1.77 (m, 1H), 1.70 – 1.55 (m, 1H). MS (ESI) m/z 606.3[M+H]⁺ and 604.2 [M-H]⁻.
6
7

8 **5-(2-{2-Methyl-5-[4-(4-methyl-piperazin-1-ylmethyl)-benzoylamino]-phenyl}-ethyl)-1H-**
9
10 **pyrrolo[2,3-*b*]pyridine-2-carboxylic acid methyl ester (28x)**

11
12 The reaction was carried out as described in general procedure C using **19a** (100 mg, 0.32
13 mmol), 4-[(4-methyl-1-piperazinyl)methyl]benzoic acid **5x** (129 mg, 0.55 mmol), HATU (148
14 mg, 0.39 mmol), DIEA (168 μ L, 0.97 mmol) and anhydrous DMF (2 mL). Purification by
15 reverse phase flash chromatography (H₂O/ACN with 1% TFA, 100/0 to 0/100) yielded after
16 neutralization with NaHCO_{3(aq)} and filtration **28x** (72 mg, 42%). ¹H-NMR (300 MHz, DMSO-*d*₆)
17 δ 12.41 (s, 1H), 10.08 (s, 1H), 8.32 (s, 1H), 7.97 (s, 1H), 7.90 (d, *J* = 7.8 Hz, 2H), 7.64 (s, 1H),
18 7.53 (d, *J* = 8.4 Hz, 1H), 7.43 (d, *J* = 7.8 Hz, 2H), 7.20 – 7.02 (m, 2H), 3.87 (s, 3H), 3.52 (s, 2H),
19 3.04 – 2.80 (m, 4H), 2.50 – 2.20 (m, 8H), 2.22 (s, 3H), 2.15 (s, 3H). MS (ESI) m/z 526.3[M+H]⁺
20 and 524.2 [M-H]⁻.
21
22
23
24
25
26
27
28
29
30
31
32
33

34 **5-(2-{5-[4-(3-Dimethylamino-pyrrolidin-1-ylmethyl)-3-trifluoromethyl-benzoylamino]-2-**
35 **methyl-phenyl}-ethyl)-1H-pyrrolo[2,3-*b*]pyridine-2-carboxylic acid methyl ester (28y)**

36
37 The reaction was carried out as described in general procedure C using **19a** (40 mg, 0.13
38 mmol), 4-(3-dimethylamino-pyrrolidin-1-ylmethyl)-3-trifluoromethyl-benzoic acid **5y** (42 mg,
39 0.13 mmol), HATU (50 mg, 0.13 mmol), DIEA (106 μ L, 0.61 mmol) and anhydrous DMF (1.5
40 mL). Purification by reverse phase flash chromatography (H₂O/ACN with 1% TFA, 100/0 to
41 0/100) yielded after neutralization with NaHCO_{3(aq)} and filtration **28y** (30 mg, 38%). ¹H-NMR
42 (300 MHz, DMSO-*d*₆) δ 12.40 (s, 1H), 10.32 (s, 1H), 8.32 (s, 1H), 8.25 – 8.18 (m, 2H), 7.97 (s,
43 1H), 7.89 (d, *J* = 8.0 Hz, 1H), 7.61 (s, 1H), 7.55 (d, *J* = 8.0 Hz, 1H), 7.17 – 7.08 (m, 2H), 3.87 (s,
44 3H), 3.86 – 3.69 (m, 2H), 3.00 – 2.85 (m, 4H), 2.81 – 2.52 (m, 4H), 2.43 – 2.33 (m, 1H), 2.23 (s,
45
46
47
48
49
50
51
52
53
54
55
56
57
58
59
60

1
2
3 3H), 2.09 (s, 6H), 1.96 – 1.80 (m, 1H), 1.77 – 1.57 (m, 1H). MS (ESI) m/z 608.3 $[M+H]^+$ and
4
5 606.3 $[M-H]^-$. HPLC purity: 89%.

6
7
8 **N-{3-[2-(2-Acetyl-1*H*-pyrrolo[2,3-*b*]pyridin-5-yl)-ethyl]-4-methyl-phenyl}-4-(4-methyl-**
9
10 **piperazin-1-ylmethyl)-benzamide (29x)**

11
12 The reaction was carried out as described in general procedure C using **19b** (70 mg, 0.24
13 mmol), 4-[(4-methyl-1-piperazinyl)methyl]benzoic acid **5x** (112 mg, 0.48 mmol), HATU (100
14 mg, 0.26 mmol), DIEA (125 μ L, 0.72 mmol) and anhydrous DMF (1.5 mL). The final compound
15 **29x** (67 mg, 55%) was isolated from crude after neutralization with $\text{NaHCO}_3(\text{aq})$, washing with
16 water and filtration. $^1\text{H-NMR}$ (300 MHz, $\text{DMSO-}d_6$) δ 12.16 (s, 1H), 10.07 (s, 1H), 8.32 (d, $J =$
17 1.9 Hz, 1H), 7.98 (d, $J = 1.8$ Hz, 1H), 7.90 (d, $J = 8.2$ Hz, 2H), 7.63 (d, $J = 1.8$ Hz, 1H), 7.53 (dd,
18 $J = 2.0, 8.2$ Hz, 1H), 7.43 (d, $J = 8.2$ Hz, 2H), 7.29 (d, $J = 2.0$ Hz, 1H), 7.10 (d, $J = 8.2$ Hz, 1H),
19 3.53 (s, 2H), 3.02 – 2.83 (m, 4H), 2.55 (s, 3H), 2.48 – 2.25 (m, 8H), 2.21 (s, 3H), 2.17 (s, 3H).
20 MS (ESI) m/z 510.3 $[M+H]^+$ and 508.3 $[M-H]^-$.

21
22
23
24
25
26
27
28
29
30
31
32 **N-{3-[2-(2-Acetyl-1*H*-pyrrolo[2,3-*b*]pyridin-5-yl)-ethyl]-4-methyl-phenyl}-4-(3-**
33
34 **dimethylamino-pyrrolidin-1-ylmethyl)-3-trifluoromethyl-benzamide (29y)**

35
36 The reaction was carried out as described in general procedure C using **19b** (100 mg, 0.34
37 mmol), 4-(3-dimethylamino-pyrrolidin-1-ylmethyl)-3-trifluoromethyl-benzoic acid **5y** (119 mg,
38 0.38 mmol), HATU (143 mg, 0.38 mmol), DIEA (178 μ L, 1.02 mmol) and anhydrous DMF (2
39 mL). Purification by reverse phase flash chromatography ($\text{H}_2\text{O}/\text{ACN}$ with 1% TFA, 100/0 to
40 0/100) yielded after neutralization with $\text{NaHCO}_3(\text{aq})$ and filtration **29y** (29 mg, 14%). $^1\text{H-NMR}$
41 (300 MHz, $\text{DMSO-}d_6$) δ 12.16 (s, 1H), 10.32 (s, 1H), 8.32 (s, 1H), 8.27 – 8.18 (m, 2H), 7.98 (s,
42 1H), 7.89 (d, $J = 7.9$ Hz, 1H), 7.61 (s, 1H), 7.54 (d, $J = 8.1$ Hz, 1H), 7.29 (s, 1H), 7.13 (d, $J =$
43 8.1 Hz, 1H), 3.88 – 3.70 (m, 2H), 2.99 – 2.84 (m, 5H), 2.72 – 2.52 (m, 3H), 2.45 – 2.38 (m, 1H),
44
45
46
47
48
49
50
51
52
53
54
55
56
57
58
59
60

1
2
3 2.22 (s, 3H), 2.16 (s, 6H), 2.00 – 1.84 (m, 1H), 1.76 – 1.62 (m, 1H). MS (ESI) m/z 592.3[M+H]⁺
4
5 and 590.2 [M-H]⁻.
6
7

8 **Modeling Studies**

9
10 The docking files (ligand + protein active site) were prepared for Autodock Vina software²⁰ by
11 using AutoDock Tools (v1.5.6).²¹ The following parameters were adjusted in this preparation
12 step: (1) the Gastieger charges and polar hydrogens were added; (2) the grid-box dimensions
13 were set at 16 Å (X), 16 Å (Y) and 28 Å (Z) in the three-space dimensions; and (3) the center of
14 the box was positioned at the midpoint of the active site, and the box volume covered the entire
15 active site area plus a significant portion of the solvent-exposed surface of the protein.
16
17
18
19
20
21
22
23

24 The following docking parameters were used in Autodock Vina: (1) all bonds in the inhibitor
25 structures were allowed to rotate freely, except for the multiple bonds, amide bonds and the
26 bonds in aromatic entities; (2) the kinase 3D structures were considered to be rigid; (3) a
27 Lamarckian genetic algorithm was used for searching the conformational space in the active site;
28 (4) the default grid spacing was set at 0.375 Å; (5) 100 different conformations were assessed,
29 and the 20 highest scored binding modes were maintained for visual inspection; (6) the
30 maximum energy difference between the best and the worst binding modes was set at 3 kcal/mol;
31 (7) the scoring function was a stochastic global optimization method inspired chiefly by X-
32 Score.²² Visual inspection of the docking results and image building was done using PyMOL
33 software.²³
34
35
36
37
38
39
40
41
42
43
44
45
46
47

48 ***In vitro* Kinase Assays**

49
50 *In vitro* kinase assays were carried out by Life Technologies' SelectScreen Biochemical
51 Kinase Profiling Service. The inhibitory activity of compounds at a 100 nM concentration was
52 evaluated against each kinase using their ATP Km concentration excepted for the B-RAF kinase
53
54
55
56
57
58
59
60

1
2
3 that was incubated in the presence of a 100 μ M ATP concentration. Results reported as a percent
4
5 of inhibition in the Tables are the mean of duplicate points. For IC₅₀ evaluation, the results were
6
7 evaluated with 10 duplicate concentration points.
8
9

10 **Proliferation Assays**

11
12 HUVEC (Human Umbilical Endothelial Vein Cells, obtained from Lonza) and HRMEC
13
14 (Human Retinal Microvascular Endothelial Cells, obtained from Angio-Proteomie) primary cells
15
16 were used at a passage less than 8 and cultured in EndoGRO-VEGF Complete Medium (Merck-
17
18 Millipore). A549, HT29, HepG2, PC-3, MDA-MB-231, Caki-2, and BxPC3 cell lines were
19
20 obtained from the European Collection of Cell Culture, the NCI-H1975 cell line was obtained
21
22 from the American Type Culture Collection, and BaF3 cells were kindly provided by Dr. J.M.
23
24 Pasquet. Cell lines were maintained in DMEM or RPMI media, each complemented with 10%
25
26 fetal bovine serum and incubated at 37°C in 5% CO₂. Human PBMC were freshly isolated by
27
28 Ficoll from 2 healthy donors and cultured with RPMI medium complemented with 10% fetal
29
30 bovine serum. PBMC were activated by adding phytohemagglutinin (PHA, 5 μ g/mL) and IL-2
31
32 (40U/mL) in cell culture medium from 48 hours before the assay. In 96-well plates, cells were
33
34 distributed at 5x10³ cells/well or 1x10⁴ cells/well depending on the doubling time of the cell type
35
36 except for human PBMC that were plated at 7.5x10⁴ cells/well. The day after plating, cells were
37
38 incubated with escalating concentrations of compounds in duplicate for 72 hours. Cell
39
40 proliferation was measured using MTT (3[4,5-dimethylthiazol-2-yl]-2,5-diphenyltetrazolium
41
42 bromide). The EC₅₀ values were calculated with 6 duplicate concentration points from
43
44 sigmoidal dose-response curves utilizing Prism 5.0 from Graph-Pad Software, with values
45
46 normalized to the values of DMSO-treated control wells (0%) and 1% SDS control wells
47
48 (100%).
49
50
51
52
53
54
55
56
57
58
59
60

Pharmacokinetics

The pharmacokinetic profile of **6z** was assessed in Swiss male mice, 5 weeks old, after single intravenous injection at 2 mg/kg (IV) or oral dosing at 20 mg/kg (PO) using DMSO as vehicle. Blood samples were collected at various time points and the compound concentrations in plasma were determined by an internal standard LC/MS/MS method using protein precipitation and calibration standards prepared in blank mouse plasma. Reported concentrations are average values from 2-mice/time point/dose group.

hERG patch clamp assay

The effects of **6z** on the hERG ion channel were measured by CytoCentrics Bioscience GmbH (Germany) according to the conventional (manual) patch clamp technique. Quality-assured HEK 293 cells stably expressing the hERG channel were used. Compound **6z** was applied at 3 concentrations (3, 10 and 30 μ M, 0.1% DMSO) using a slow perfusion system with a tube pump. Each compound concentration was tested on two individual cells. Cisapride was used as reference compound at a concentration of 200 nM to induce a hERG tail current inhibition and to validate the experiment.

ASSOCIATED CONTENT

Supporting Information. Homology modeling and docking studies. Details of HPLC methods used for purity determination, HPLC purities and NMR spectra. This material is available free of charge *via* the Internet at <http://pubs.acs.org>.

PDB ID Codes: 1UWH, 2OIQ, 4ASD, 1IEP, 3VNT, 4RT7.

AUTHOR INFORMATION

Corresponding Author

*E-mail: ayasri@oribase-pharma.com. Phone: (+33) 467 727 670.

Author Contributions

The manuscript was written through contributions of all authors. All authors have given approval to the final version of the manuscript.

Funding Sources

The research was supported by OriBase Pharma.

ACKNOWLEDGMENT

The authors thank Dr. Jean-Max Pasquet for providing cell lines and Dr. Francisco Veas and Gregor Dubois for laboratory assistance and discussions.

ABBREVIATIONS

MTKI, multi-targeted kinase inhibitor; MAPK, mitogen-activated protein kinase; PI3K, phosphoinositide 3-kinase; PDB, Protein Data Bank; PBP, purine binding pocket; SP, selectivity pocket I; EGFR, Epidermal Growth Factor Receptor; VEGFR2, Vascular Endothelial Growth Factor Receptor 2; FGFR2, Fibroblast Growth Factor Receptor 2; PDGFRA, Platelet-Derived Growth Factor Receptor alpha; rt, room temperature; aq, aqueous; nd, not determined; ACN, acetonitrile; FA, formic acid

REFERENCES

- (1) Zhang, J.; Yang, P. L.; Gray, N. S. Targeting Cancer with Small Molecule Kinase Inhibitors. *Nat. Rev. Cancer* **2009**, *9* (1), 28–39.
- (2) Knapp, S.; Sundström, M. Recently Targeted Kinases and Their Inhibitors — the Path to Clinical Trials. *Curr. Opin. Pharmacol.* **2014**, *17*, 58–63.

- 1
2
3
4
5
6
7
8
9
10
11
12
13
14
15
16
17
18
19
20
21
22
23
24
25
26
27
28
29
30
31
32
33
34
35
36
37
38
39
40
41
42
43
44
45
46
47
48
49
50
51
52
53
54
55
56
57
58
59
60
- (3) Gerlinger, M.; Rowan, A. J.; Horswell, S.; Larkin, J.; Endesfelder, D.; Gronroos, E.; Martinez, P.; Matthews, N.; Stewart, A.; Tarpey, P.; Varela, I.; Phillimore, B.; Begum, S.; McDonald, N. Q.; Butler, A.; Jones, D.; Raine, K.; Latimer, C.; Santos, C. R.; Nohadani, M.; Eklund, A. C.; Spencer-Dene, B.; Clark, G.; Pickering, L.; Stamp, G.; Gore, M.; Szallasi, Z.; Downward, J.; Futreal, P. A.; Swanton, C. Intratumor Heterogeneity and Branched Evolution Revealed by Multiregion Sequencing. *N. Engl. J. Med.* **2012**, *366* (10), 883–892.
- (4) Klein, C. A. Selection and Adaptation during Metastatic Cancer Progression. *Nature* **2013**, *501* (7467), 365–372.
- (5) Gossage, L.; Eisen, T. Targeting Multiple Kinase Pathways: A Change in Paradigm. *Clin. Cancer Res. Off. J. Am. Assoc. Cancer Res.* **2010**, *16* (7), 1973–1978.
- (6) Dar, A. C.; Das, T. K.; Shokat, K. M.; Cagan, R. L. Chemical Genetic Discovery of Targets and Anti-Targets for Cancer Polypharmacology. *Nature* **2012**, *486* (7401), 80–84.
- (7) Knight, Z. A.; Lin, H.; Shokat, K. M. Targeting the Cancer Kinome through Polypharmacology. *Nat. Rev. Cancer* **2010**, *10* (2), 130–137.
- (8) Chev e, G.; Bories, C.; Fauvel, B.; Picot, F.; Tible, A.; Dayd e-Cazals, B.; Loget, O.; Yasri, A. De Novo Design, Synthesis and Pharmacological Evaluation of New Azaindole Derivatives as Dual Inhibitors of Abl and Src Kinases. *MedChemComm* **2012**, *3* (7), 788–800.
- (9) Fauvel, B.; Coisy-Quivy, M.; Vivier, S.; Chev e, G.; Bori es, C.; Dayd e-Cazals, B.; Feneyrolles, C.; Bestgen, B.; Delon, L.; Dufies, M.; Auberger, P.; Loget, O.; Yasri, A. Anti-Tumor Activity of Novel Compounds Targeting BCR-ABL, c-SRC and BCR-ABL T315I in Chronic Myelogenous Leukemia. *Am. J. Cancer Sci.* **2013**, *2* (1), 28–36.

- 1
2
3
4
5
6
7
8
9
10
11
12
13
14
15
16
17
18
19
20
21
22
23
24
25
26
27
28
29
30
31
32
33
34
35
36
37
38
39
40
41
42
43
44
45
46
47
48
49
50
51
52
53
54
55
56
57
58
59
60
- (10) Getlik, M.; Grütter, C.; Simard, J. R.; Klüter, S.; Rabiller, M.; Rode, H. B.; Robubi, A.; Rauh, D. Hybrid Compound Design to Overcome the Gatekeeper T338M Mutation in cSrc. *J. Med. Chem.* **2009**, *52* (13), 3915–3926.
- (11) Seeliger, M. A.; Nagar, B.; Frank, F.; Cao, X.; Henderson, M. N.; Kuriyan, J. C-Src Binds to the Cancer Drug Imatinib with an Inactive Abl/c-Kit Conformation and a Distributed Thermodynamic Penalty. *Struct. Lond. Engl. 1993* **2007**, *15* (3), 299–311.
- (12) Nagar, B.; Bornmann, W. G.; Pellicena, P.; Schindler, T.; Veach, D. R.; Miller, W. T.; Clarkson, B.; Kuriyan, J. Crystal Structures of the Kinase Domain of c-Abl in Complex with the Small Molecule Inhibitors PD173955 and Imatinib (STI-571). *Cancer Res.* **2002**, *62* (15), 4236–4243.
- (13) Choi, H. G.; Ren, P.; Adrian, F.; Sun, F.; Lee, H. S.; Wang, X.; Ding, Q.; Zhang, G.; Xie, Y.; Zhang, J.; Liu, Y.; Tuntland, T.; Warmuth, M.; Manley, P. W.; Mestan, J.; Gray, N. S.; Sim, T. A Type-II Kinase Inhibitor Capable of Inhibiting the T315I “Gatekeeper” Mutant of Bcr-Abl. *J. Med. Chem.* **2010**, *53* (15), 5439–5448.
- (14) Koroleva, E. V.; Kadutskii, A. P.; Farina, A. V.; Ignatovich, J. V.; Ermolinskaya, A. L.; Gusak, K. N.; Kalinichenko, E. N. A Practical Synthesis of 4-[(4-Methylpiperazin-1-yl)methyl]benzoic Acid—the Key Precursor toward Imatinib. *Tetrahedron Lett.* **2012**, *53* (38), 5056–5058.
- (15) Gwénaél Chevé; Bénédicte Daydé-Cazals; Bénédicte Fauvel; Cédric Boriès; Abdelaziz Yasri. NEW AZAINDOLE DERIVATIVES AS INHIBITORS OF PROTEIN KINASES. WO2014102378 A1.
- (16) Pessina, A.; Malerba, I.; Gribaldo, L. Hematotoxicity Testing by Cell Clonogenic Assay in Drug Development and Preclinical Trials. *Curr. Pharm. Des.* **2005**, *11* (8), 1055–1065.

- 1
2
3
4
5
6
7
8
9
10
11
12
13
14
15
16
17
18
19
20
21
22
23
24
25
26
27
28
29
30
31
32
33
34
35
36
37
38
39
40
41
42
43
44
45
46
47
48
49
50
51
52
53
54
55
56
57
58
59
60
- (17) Hassan, S. B.; Haglund, C.; Aleskog, A.; Larsson, R.; Lindhagen, E. Primary Lymphocytes as Predictors for Species Differences in Cytotoxic Drug Sensitivity. *Toxicol. Vitro Int. J. Publ. Assoc. BIBRA* **2007**, *21* (6), 1174–1181.
- (18) Schade, A. E.; Schieven, G. L.; Townsend, R.; Jankowska, A. M.; Susulic, V.; Zhang, R.; Szpurka, H.; Maciejewski, J. P. Dasatinib, a Small-Molecule Protein Tyrosine Kinase Inhibitor, Inhibits T-Cell Activation and Proliferation. *Blood* **2008**, *111* (3), 1366–1377.
- (19) Lee, K. C.; Ouwehand, I.; Giannini, A. L.; Thomas, N. S.; Dibb, N. J.; Bijlmakers, M. J. Lck Is a Key Target of Imatinib and Dasatinib in T-Cell Activation. *Leukemia* **2010**, *24* (4), 896–900.
- (20) Trott, O.; Olson, A. J. AutoDock Vina: Improving the Speed and Accuracy of Docking with a New Scoring Function, Efficient Optimization, and Multithreading. *J. Comput. Chem.* **2010**, *31* (2), 455–461.
- (21) Goodsell, D. S.; Olson, A. J. Automated Docking of Substrates to Proteins by Simulated Annealing. *Proteins* **1990**, *8* (3), 195–202.
- (22) Wang, R.; Lai, L.; Wang, S. Further Development and Validation of Empirical Scoring Functions for Structure-Based Binding Affinity Prediction. *J. Comput. Aided Mol. Des.* **2002**, *16* (1), 11–26.
- (23) The PyMol Molecular Graphics System, Version 0.99rc6, Schrodinger, LLC.

Table of Contents Graphic

